

Novae in M51: a New, Much Higher Rate from Multi-epoch HST Data

Shifra Mandel,^{1*} Michael M. Shara,² David Zurek² Charlie Conroy³ and Pieter van Dokkum⁴

¹*Columbia Astrophysics Laboratory, Columbia University, New York, NY 10027, USA*

²*Department of Astrophysics, American Museum of Natural History, New York, NY, USA*

³*Department of Astronomy, Harvard University, Cambridge, MA, 02138, USA*

⁴*Department of Astronomy, Yale University, New Haven, CT, 06511, USA*

Accepted 2022 September 27. Received 2022 September 26; in original form 2022 August 24

ABSTRACT

Accurate determination of the rates of nova eruptions in different kinds of galaxies give us strong constraints on those galaxies’ underlying white dwarf and binary populations, and those stars’ spatial distributions. Until 2016, limitations inherent in ground-based surveys of external galaxies – and dust extinction in the Milky Way – significantly hampered the determination of those rates and how much they differ between different types of galaxies. Infrared Galactic surveys and dense cadence *Hubble Space Telescope* (*HST*)-based surveys are overcoming these limitations, leading to sharply increased nova-in-galaxy rates relative to those previously claimed. Here we present 14 nova candidates that were serendipitously observed during a year-long *HST* survey of the massive spiral galaxy M51 (the “Whirlpool Galaxy”). We use simulations based on observed nova light curves to model the incompleteness of the *HST* survey in unprecedented detail, determining a nova detection efficiency $\epsilon = 20.3$ percent. The survey’s M51 area coverage, combined with ϵ , indicates a conservative M51 nova rate of 172_{-37}^{+46} novae yr⁻¹, corresponding to a luminosity-specific nova rate (LSNR) of $\sim 10.4_{-2.2}^{+2.8}$ novae yr⁻¹/10¹⁰L_{⊙,K}. Both these rates are approximately an order of magnitude higher than those estimated by ground-based studies, contradicting claims of universal low nova rates in all types of galaxies determined by low cadence, ground-based surveys. They demonstrate that, contrary to theoretical models, the *HST*-determined LSNR in a giant elliptical galaxy (M87) and a giant spiral galaxy (M51) likely do *not* differ by an order of magnitude or more, and may in fact be quite similar.

Key words: nova, cataclysmic variables – galaxies: stellar content – supernovae: general

1 INTRODUCTION

All cataclysmic variables (CVs) are binaries containing a white dwarf (WD) which accretes matter from a close companion. A nova eruption is a bright (up to 10⁶ L_⊙) outburst that occurs when the envelope accreted onto the WD surface ignites in a thermonuclear runaway. Nova characteristics (such as the recurrence rate, peak luminosity, and decay time) encode information about the WD and donor star, as well as the binary mass transfer rate during the millenia between nova eruptions (Hillman et al. 2016, 2020). Novae are our only means of studying CV populations (and indeed most binary populations) in galaxies beyond the Local Group. In addition, the most rapidly accreting WDs in nova binaries can be progenitors of “standard candle” type Ia supernovae (SNIa) (Hillman et al. 2016), so these stars’ importance extends beyond the domain of stellar evolution to cosmology.

Given that CVs with high accretion rates from sub-giant companions and/or very massive WDs are likely SNIa progenitors (Hillman et al. 2016), the dependence of CV populations on the underlying stellar populations and the environments of their host galaxies is of great importance for determining whether SNIa are reliable standard candles. Varying CV populations in different galaxy types could be an indicator of differing SNIa progenitor channels, with

important implications for the determination of the Hubble constant H_0 using SNIa as distance indicators. Differences in CV populations could also hint at different binary fractions and/or stellar evolution pathways in different types of galaxies.

Despite their importance in understanding and testing models of binary stellar evolution, and implications for cosmological standard candles, a lack of consensus on the actual nova rates in galaxies has persisted for two decades. On the basis of multiple ground-based surveys, Shafter et al. (2000) and Shafter et al. (2014) claimed that the luminosity specific nova rates (LSNR, i.e. annual rate of novae per unit K-band luminosity) in different galaxy types are all similar, in the range of 1–3 novae yr⁻¹/10¹⁰L_{⊙,K}. In contrast, the population synthesis studies of Matteucci et al. (2003), Claeys et al. (2014) and Chen et al. (2016) suggested that order-of-magnitude differences in nova rates and LSNR should exist between elliptical, spiral, and especially starburst galaxies. This is because rapid and massive star formation should produce a plethora of mass-transferring binaries containing high-mass WDs in spiral and starburst galaxies. Novae which erupt on high-mass WDs do so after accreting relatively low-mass envelopes (Yaron et al. 2005). Such novae can thus erupt more frequently than those associated with low mass WDs, so that the LSNR in spiral and especially in starburst galaxies are predicted to greatly exceed the corresponding rates in elliptical galaxies.

Using a *Hubble Space Telescope* (*HST*) survey of the massive elliptical galaxy M87, Shara et al. (2016) showed that ground-based sur-

* E-mail: ss5018@columbia.edu

veys of external galaxies fail to detect fainter novae and/or those with short decline times and/or those near the bright centers of galaxies. These effects cause ground-based surveys to systematically underestimate the true nova rates in galaxies. In the case of M87, these effects led to the ground-based underestimate of the M87 nova rate by a factor of 2-4; the *HST*-determined LSNR in the K-band was shown to be $7.88^{+2.3}_{-2.6}$ novae yr⁻¹/10¹⁰ L_{⊙,K} (Shara et al. 2016). Confirmation of ground-based nova rate underestimates was provided by Mróz et al. (2016), who demonstrated that the LSNR in the Large Magellanic Cloud (LMC) is much higher than previous ground-based estimates, and is comparable to the M87 LSNR. This finding was further supported by De et al. (2021), who discovered a sizable population of Galactic novae (in the infrared) that have gone undetected in over a century of optical searches, and Kawash et al. (2021), who found that approximately half of all Galactic novae are hidden from current surveys by extinction.

These discoveries (of much higher than previously claimed LSNR) in a giant elliptical (M87), a barred spiral (the Galaxy), and a dwarf irregular galaxy (LMC), were carried out via surveys with much longer baselines, denser time coverage and/or deeper magnitude limits than all previous surveys. They argue strongly against the claim that the LSNR is relatively low in all galaxies, as the earlier, shallower and sparser cadence coverage of Shafter et al. (2000) and Shafter et al. (2014) suggested. They highlight the need for deep, unbiased surveys of other types of galaxies to confirm that the LSNRs are much higher than previously thought, and to test whether they vary with galaxy type, as predicted by binary population synthesis models. In particular, a giant Sc-type spiral galaxy has not yet been so studied. *HST* is especially suited to such investigations because of its unparalleled angular resolution and consequent sensitivity, its very small and virtually constant point-spread function, its insensitivity to lunar phase and its immunity to atmospheric seeing.

The massive Sc-type spiral galaxy M51 (the Whirlpool Galaxy, NGC 5194) has been surveyed for novae only once, over 20 years ago (Shafter et al. 2000). Narrowband *Hα* and broadband *R* images centered on M51, and covering 16'x16' (the entire galaxy), were taken with the Kitt Peak National Observatory 4-meter telescope at four well-separated epochs in 1994 and 1995. These data led to the discovery of nine novae. Allowing for gaps in coverage and other sources of incompleteness (such as a limiting absolute magnitude detection limit of -7.7 ± 0.22), Shafter et al. (2000) derived a rate of 18 ± 7 novae yr⁻¹ in M51. This corresponds to an M51 LSNR of 1.09 ± 0.47 novae yr⁻¹/10¹⁰ L_{⊙,K}.

M51 was the subject of an *HST* observing campaign that began in 2016 and continued for nearly a year (Conroy et al. 2018). The stated goal of that survey was to catalog and categorize all luminous stellar variables within a significant fraction of that galaxy. Given its optimal orientation on the sky – M51 is face-on, which minimizes internal reddening, and benefits from a fairly low Galactic extinction that is approximately constant across the field – this survey also offers an excellent opportunity for the most complete and unbiased study of the novae in a massive Sc-type spiral galaxy to date. Although the irregular cadence and sometimes weeks-long gaps between observations of M51 are not ideal for a nova survey, the proximity of M51 (relative to M87) allows us to detect novae in *HST* images even if they are intrinsically faint (hence much too faint to detect from the ground) and/or after they have dimmed several magnitudes from maximum light. In particular, the archival *HST* imaging dataset of M51 enables just the second, head-to-head comparison (after M87) of ground-based versus *HST*-derived nova rates in the same galaxy.

Section 2 describes the data collected during the M51 *HST* observing campaign. Section 3 describes our search for and identification

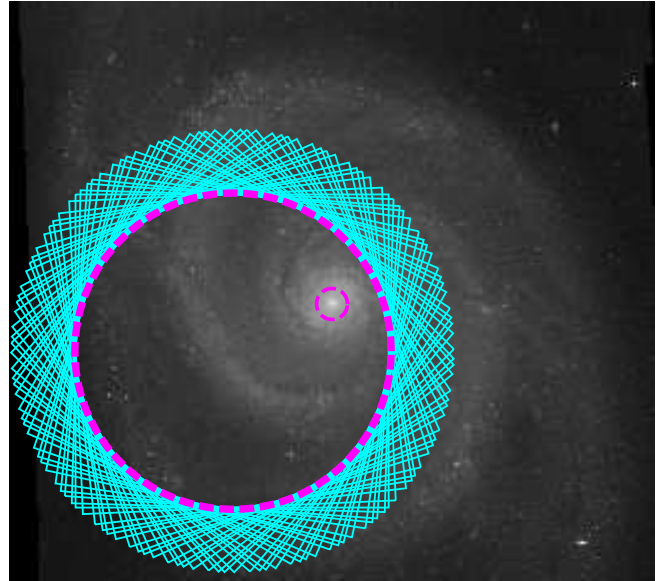


Figure 1. *HST* ACS I_{814} -band mosaic of M51. The footprints of the 34 observations used for this study are shown in cyan; the large dashed magenta circle marks the region consistently observed and included in the photometric data.

of nova candidates and their properties. In Section 4 and in section 5 we describe the details of the simulations we conducted to investigate, respectively, the detection efficiency and the incompleteness of our *HST* survey. In Section 6 we discuss our findings and their implications, and we summarize our results in Section 7.

2 *HST* IMAGING DATA

The *HST* observing campaign of M51 was conducted over the course of 345 days using the Advanced Camera for Surveys (ACS) Wide-Field Channel (WFC) F_{606W} and F_{814W} filters (hereafter V_{606} and I_{814} , respectively). Each of the 34 imaging epochs, with a total 2.2 ksec exposure in each of the V_{606} and I_{814} bands, covered ~ 40 percent of the galaxy's I_{814} flux (see Section 6.1). While the *average* gap between observations was ~ 10 days, the survey cadence ranged from 4 to 24 days. Figure 1 shows the *HST* fields of view (FOV) of those 34 epochs. Note that the FOVs rotate to maintain optimal pointing of *HST*'s solar panels throughout the course of the year. We considered only the portion of the FOVs that was covered in every epoch (see Figure 3 for more details).

To create the M51 star catalog, point-spread-function (PSF) photometry was performed using the DOLPHOT software package (Dolphin 2000; Conroy et al. 2018). The regions around six bright foreground stars were masked to avoid contamination. The central 10 arcsec were also excluded, because the region is extremely crowded, making PSF photometry impracticable. A detailed description of the observations and the methods used to extract the photometric data are given in Conroy et al. (2018). In total, the *HST* data yielded photometric measurements at 34 epochs in two passbands for ~ 1.39 million stars.

The survey's magnitudes are on the Vega zero point (*VEGAMAG*) system. All absolute magnitudes were computed assuming an M51 distance modulus of 29.67 with Galactic extinctions in the direction of M51 of $A_{606} = 0.086$ and $A_{814} = 0.053$ mag (McQuinn et al. 2016).

Table 1. Nova Candidates in M51

Nova	M51 Nucleus Offset [arcsec]	RA (J2000) [deg]	DEC (J2000) [deg]	M_{peak} (V_{606})	M_{peak} (I_{814})	$t_{peak,V}$ [MJD]
1	74.31	202.49935	47.19936	-8.51	-8.97	57675
2	10.77	202.46526	47.19466	-7.99	-8.28	57936
3	23.36	202.46145	47.19867	-7.79	-8.27	57971
4	114.87	202.48422	47.16494	-7.78	-8.04	57858
5	15.55	202.47586	47.19589	-7.73	-8.26	57946
6	45.85	202.48117	47.18525	-7.26	-7.68	57971
7	30.26	202.45930	47.19994	-7.07	-7.33	57666
8	33.21	202.47781	47.18792	-6.97	-7.42	57666
9	119.21	202.51632	47.20461	-6.89	-7.22	57760
10	54.92	202.48981	47.20186	-6.72	-7.34	57993
11	47.62	202.48200	47.20544	-6.41	-7.41	57760
12	67.81	202.49248	47.18465	-6.17	-6.48	57699
13	94.0	202.47425	47.16934	-6.03	-6.91	57925
14	22.89	202.47877	47.19641	-5.53	-6.50	57666

Fourteen nova candidates discovered in the *HST* observations of M51, listed in order of observed peak luminosity.

3 M51 NOVA SEARCH AND IDENTIFICATION

The four defining characteristics we used to identify potential M51 nova candidates (cf. [Shara et al. \(2016\)](#)) among the ~ 1.39 million stars in the *HST* dataset are:

- a peak absolute magnitude brighter than -5 in the V_{606} and I_{814} bands,
- a decrease from peak brightness of at least 2 mag over the duration of the observing campaign,
- a “blue” color (average near maximum light) of $V_{606} - I_{814} < 0.50$ mag, and
- no apparent periodic variability.

These criteria are satisfied by virtually all known novae, and are deliberately over-conservative so as not to miss any reasonably identifiable candidates on a first pass. Approximately 1,000 preliminary nova candidates were selected using the above parameter and light curve constraints. Every candidate’s light curve was visually inspected, allowing us to weed out eclipsing, periodic, and spurious sources. [A number of discarded sources could have been either novae or other highly variable (and similarly “blue”-colored) stars, like cepheids or luminous blue variables (LBVs). We retained only sources that showed the canonical single-peaked fast rise and exponential decline that is most often observed in novae, but not in other highly variable stars, although nova light curves can take a variety of shapes ([Strope et al. 2010](#)).] All surviving candidates were visually inspected in the *HST* images. Fourteen final nova candidates remained.

Table 1 lists the 14 nova candidates we identified in the *HST* dataset, including their angular offsets from M51’s nucleus, J2000 coordinates, absolute magnitudes (V_{606} - and I_{814} -band) at maximum light, and the date of observed maximum brightness. (Note that the actual peak luminosity for these nova outbursts could have been higher by up to several magnitudes; because of the gaps between *HST* observations, most were likely detected during their decline.) We deliberately omit t_2 because, due to the large gaps between the *HST* observations of M51, the uncertainties in t_{peak} and M_{peak} – both of which are required to evaluate t_2 – are too great to allow for meaningful estimates of the decline time.

The light curves for the 14 novae are shown in Figure 2. “Postage stamp” difference images of all novae in Table 1 for each observing

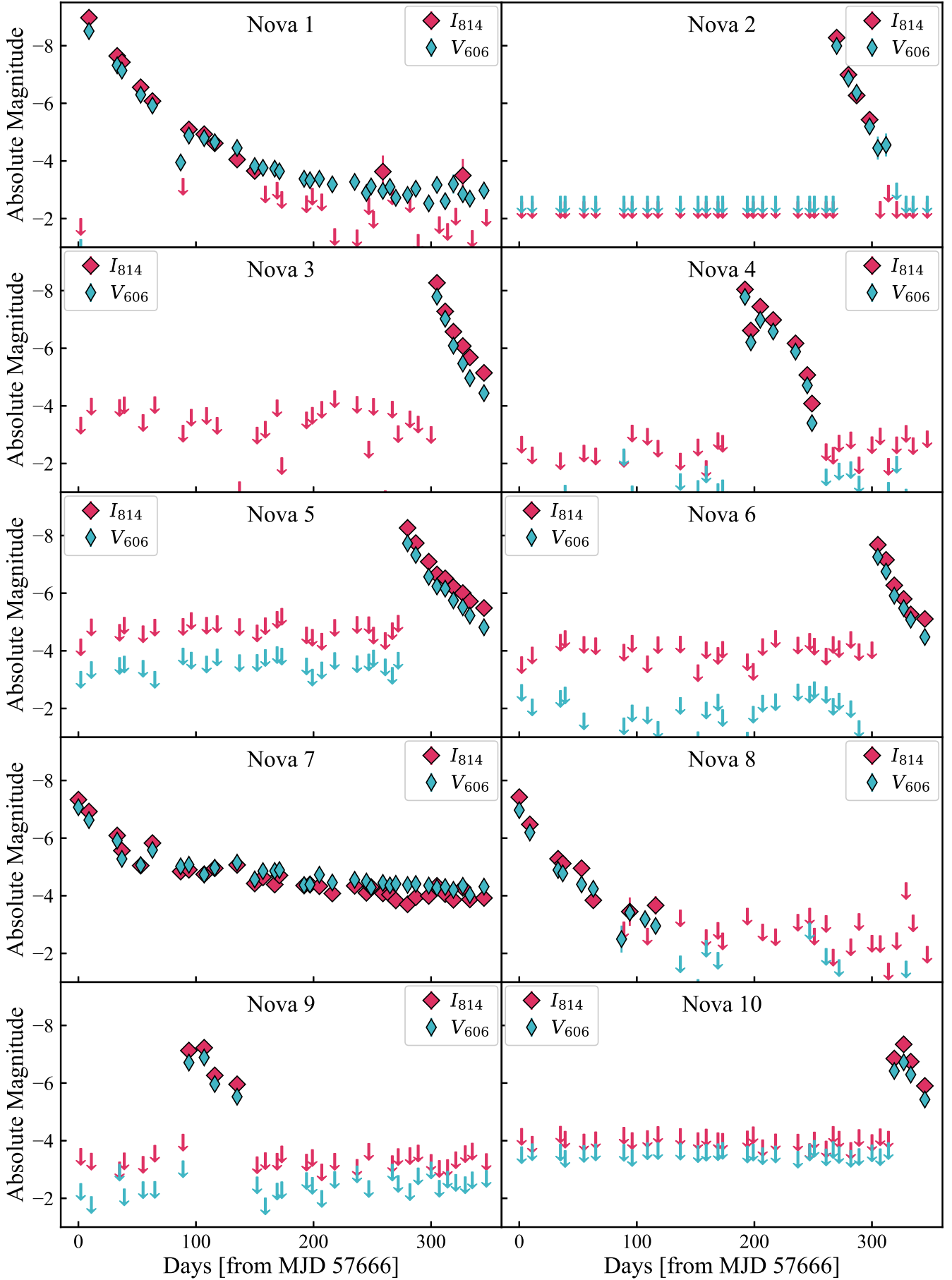
epoch are shown in Appendix B. The spatial distribution of the novae can be seen in Figure 3, in which the positions of the 14 novae are overlaid on an image of M51.

4 M51 SURVEY NOVA DETECTION EFFICIENCY

In addition to observing cadence, the observational properties that have the largest effect on whether a nova outburst will be detected or missed are that nova’s peak luminosity (M_{peak}) and the decline time. The latter is often defined as t_2 , which is the time required for the luminosity to decrease from M_{peak} by two magnitudes. The non-uniform cadence of – and large gaps between – the *HST* observations of M51 must necessarily hamper the detection of rapidly fading novae and the peak luminosities L_{peak} of most outbursts. To quantify the *detection efficiency* (ϵ) of our survey as a function of M_{peak} and t_2 (as opposed to its *incompleteness*, which we address in Section 5), we generated an idealized set of artificial novae covering essentially the entire ranges of observed nova M_{peak} and t_2 . (Not all combinations of nova M_{peak} and t_2 are observed in nature, particularly the combination of most luminous M_{peak} and longest t_2 , but their inclusion is nonetheless instructive).

We adopted M_{peak} values of $[-10, -9.75, -9.5, \dots, -5]$ mag and t_2 values of $[2, 5, 8, \dots, 152]$ days. All combinations of these 21 values of M_{peak} and 51 values of t_2 produced a total of 1,071 artificial nova light curves. Each artificial nova was assumed to decline exponentially, beginning at M_{peak} and fading through the *HST* detection threshold for the M51 survey, $V_{606} \approx 27.5$ mag. Each synthetic nova outburst was then begun at day (t_0) $[0, 1, 2, \dots, 345]$ (corresponding to the length of the *HST* observing campaign of M51) and sampled with the *HST* observing cadence. This range of outburst start times was necessary to account for biases in detectability based on the *HST* observing cadence near the eruption date, as the gap between *HST* epochs varied between 4 and 24 days throughout the campaign.

This process yielded $346 \times 1071 = 370,566$ light curves, sampled with the *HST* observing cadence. Each light curve was evaluated to determine whether the corresponding nova would have been detected as such via our V_{606} -band selection parameters, listed in Section 3. This yields the survey’s detection efficiency as a function of M_{peak}



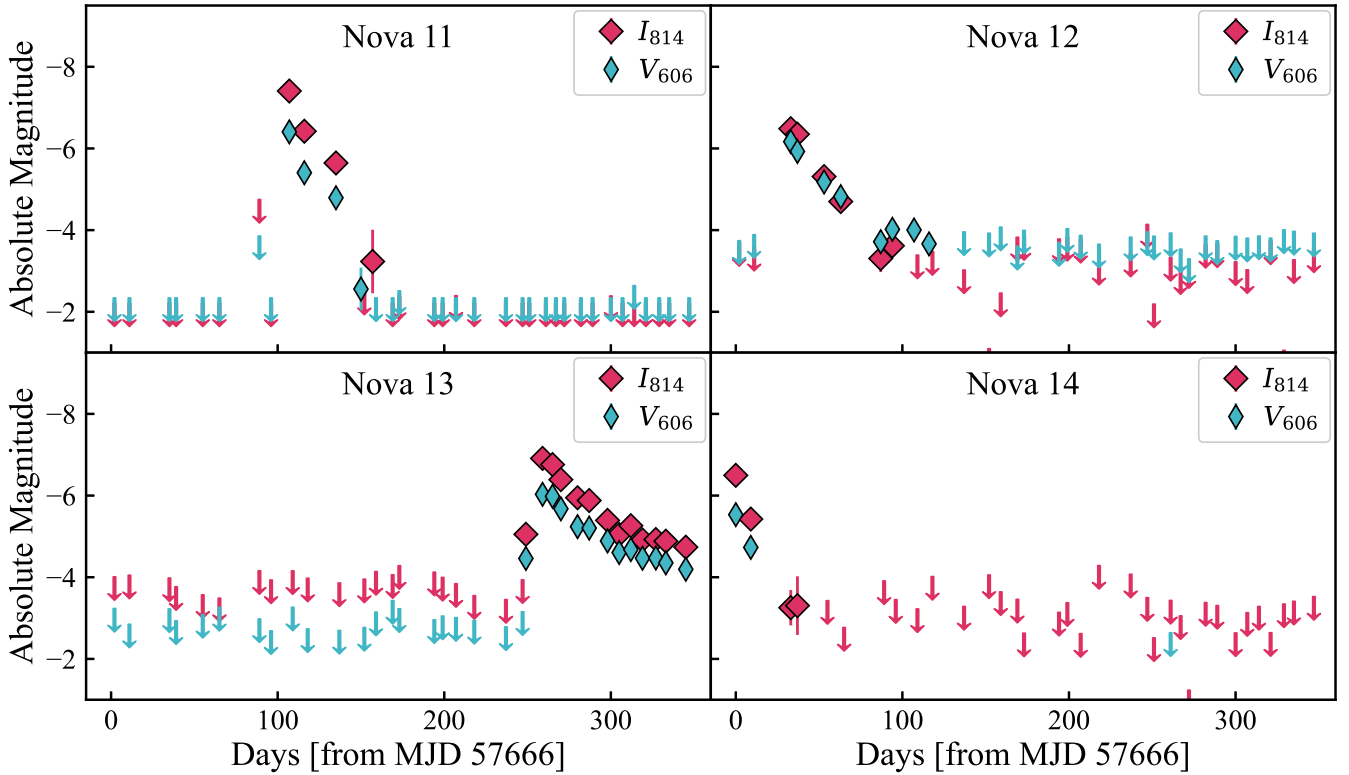


Figure 2. V_{606} - and I_{814} - band light curves (shown in blue and red, respectively) for the 14 nova candidates in M51. Arrows mark upper limits. Where no error bars are visible, magnitude errors are smaller than the data point markers.

and t_2 . The results are plotted in Figure 4. As expected, the figure demonstrates that novae with brighter M_{peak} and longer t_2 were more likely to be detected than their fainter/faster counterparts, except when their decline times (t_2) stretched to months. The latter effect is due to the decrease in observed variability when the decline time is very long.

The existence of intrinsically faint novae with small t_2 (the so-called “faint/fast novae”) was predicted in the 2005 compendium of nova models with a wide range of WD masses and accretion rates (Yaron et al. 2005). They were first detected observationally by Kasliwal et al. (2011) in M31, then by Shara et al. (2016) in M87, and are now understood to be common. Their ubiquity and importance in determining our survey’s incompleteness are apparent in Figure 4, where we overlaid the best optical samples of Galactic, M31, and M87 novae that are currently available on the detection efficiency plot just described.

If they erupted in M51, a significant fraction of all novae observed in M87, M31 and the Galaxy would nearly always be missed in the current survey because they display $t_2 < 10$ days. The poor detectability of novae with $t_2 \lesssim 10$ days in our survey is a consequence of the large gaps between the *HST* observations of M51. Many novae are observed to erupt with $t_2 \lesssim 10$ days, which, as noted above, are very difficult to detect in this survey. Conversely, almost all novae with $t_2 > 20$ days and $M_{peak} \lesssim -8$ would be detectable (assuming a simplified exponential decline shape¹). No such novae

have ever been reported, or predicted by large suites of nova models (Yaron et al. 2005). The lack of detection of any such novae in our M51 *HST* survey (despite the excellent detection efficiency associated with them) is further evidence that such objects are very rare, or do not exist.

5 INCOMPLETENESS SIMULATIONS USING OBSERVED NOVAE

To determine the nova rate in M51, we must first measure our survey’s incompleteness viz. the fraction of novae that erupted in M51 during our survey but which were not detected. While the idealized, highly simplified simulations described in Section 4 help us understand how luminosity and decline time affect the detectability of novae subject to the *HST* M51 survey cadence, the reality is more complex. This is because the *shape* of a nova light curve, which is generally *not* exponential throughout, also plays a crucial role in its detectability, as demonstrated in Figure 5. The decline of a nova’s brightness is often fastest immediately following the outburst peak, though the opposite sometimes occurs. Some novae reach a steady brightness plateau for days or weeks during their declines, while others undergo deep dips as dust forms in their ejecta. The rates of change in luminosity, and when those changes occur, vary greatly among well-sampled Galactic novae (Strope et al. 2010). Thus the irregularly spaced epochs of this survey must be convolved with a set of realistic light curves, representative of M51 novae, to determine our survey’s incompleteness.

There is no published set of well-sampled light curves of novae in M51 or in any other Sc-type galaxy. Thus we have produced a series of simulations using the three most realistic and complete sets

¹ The full range of nova light curve morphologies, including some that are considerably more complex than the simplistic models we adopt here, is detailed in Strope et al. (2010). We use those and other realistic light curves in section 5 below when we determine our survey’s incompleteness.

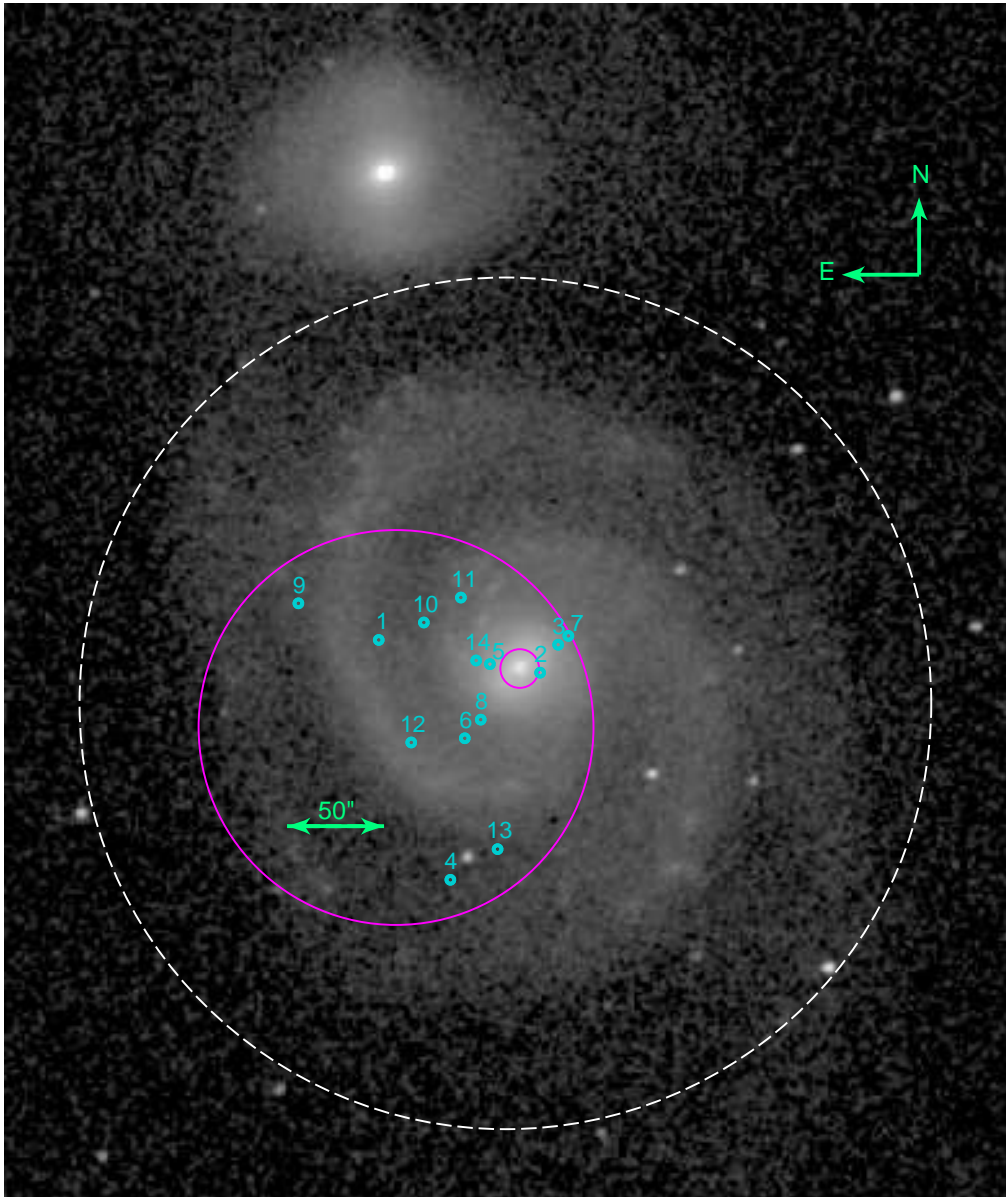


Figure 3. 2MASS K-band image showing the approximate “footprint” (cf. Figure 1) of the *HST* survey (magenta), an area of radius ~ 102 arcsec. The central 10 arcsec of M51 were excluded from our photometric analysis. The M51 light fraction covered in this survey - 40 percent - was computed with the assumption that the light inside the white circle (radius 220 arcsec) constitutes all the light from M51 (see 6.1 for more). The locations and IDs of the nova candidates we identified are shown in turquoise.

of light curves available from well-observed novae in our Galaxy, M31 and M87. A list of all novae that were used in the following simulations of 5.1 - 5.2 are found in Table A1 in Appendix A. A summary of the results is shown in table 2.

5.1 Simulation I. Galactic Novae

The largest collection of well-sampled novae starting near maximum brightness and extending well into the decline phase comprises, not surprisingly, Galactic novae. Strope et al. (2010) published the light curves of 93 Galactic novae, most of which were well monitored from outburst peak through several magnitudes of decline. Of these, 32 have well-determined distances that allow us to calculate their absolute magnitudes, either from *Gaia* parallaxes

(Schaefer 2018) or through the blackbody flux of their giant companions (Özdönmez et al. 2018).

This largest Galactic nova sample with well-calibrated luminosities is unfortunately far from unbiased. In particular, it is conspicuously lacking in faint/fast novae (Kasliwal et al. 2011; Shara et al. 2016), which were missed throughout 20th century nova searches. As Figure 4 demonstrates, our M51 survey’s detection efficiency ϵ for novae with $t_2 \lesssim 10$ days is close to zero. While we investigated whether each of these 32 Galactic novae would be identifiable as such *had it occurred within M51 during our HST observing campaign*, the lack of faint/fast novae in the Galactic sample means that its incompleteness estimate will be an upper limit only. See Section 6.3.1 for more details.

Similarly to the process for the synthetic novae, each of the above

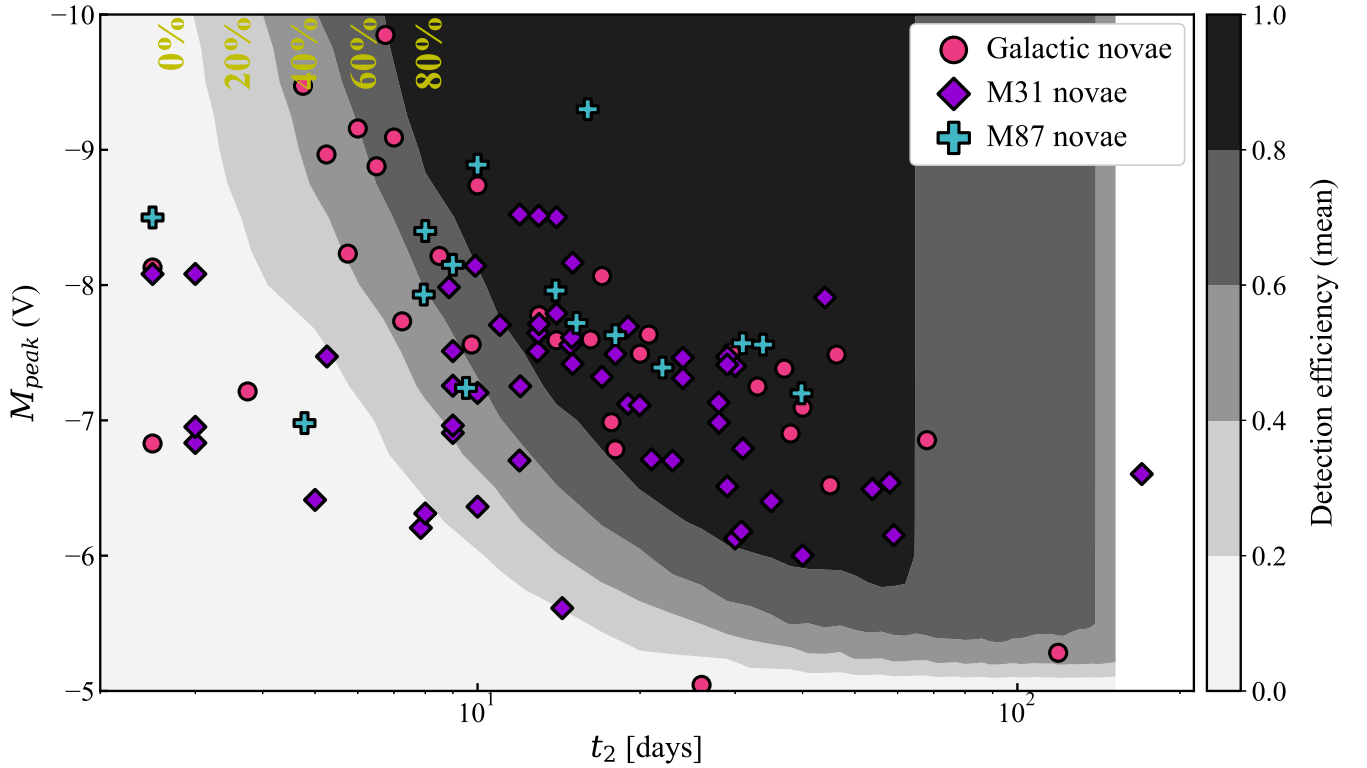


Figure 4. Detection efficiency of synthetic novae for the full range of nova M_{peak} and t_2 discussed in Section 4, sampled at the M51 *HST* observing cadence. Contours denote a 20 percent change in efficiency. Galactic, M31, and M87 novae are overlaid in pink, violet, and blue, respectively.

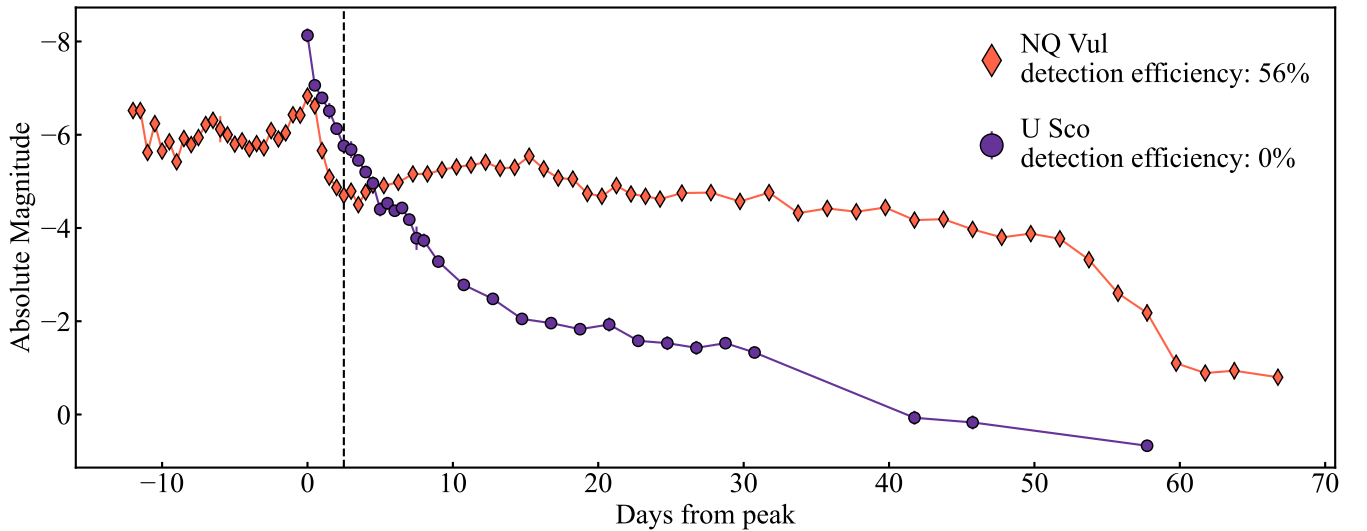


Figure 5. Light curves of two Galactic novae, NQ Vul (orange) and U Sco (purple). These novae have identical t_2 (dotted line) but different decline shapes, resulting in a lower detection efficiency in our M51 survey for the *brighter* nova (U Sco). This demonstrates the importance of modelling detection efficiency using real nova light curves, as M_{peak} and t_2 alone are not reliable predictors for detectability.

32 Galactic nova light curves was begun at $t_0 = [-20, -19, -18, \dots, 345]$ days² and sampled with the *HST* observing cadence. Lin-

² Given the overall excellent sampling frequency and extended duration of the Galactic nova light curves, we were able to model outbursts occurring over a full year, starting 20 days before the *HST* observing campaign of M51 commenced.

ear interpolation was utilized where small gaps in the Galactic nova light curves coincided with one of the M51 *HST* epochs. This provided us with a realistic set of 11,680 simulated nova light curves. Then, as we had done for the synthetic novae, we evaluated each of the simulated light curves to determine whether it would have yielded a nova detection using our V_{606} -band selection parameters, summarized in Section 2.

The results of our detection efficiency evaluations for the 32 Galactic novae with the most reliable distances are shown in the left panel of Figure 6. The M_{peak} , t_2 , and mean detection efficiency ϵ shown for each data point in Figure 6 correspond to the Galactic nova that was used to generate the simulated light curves. The mean ϵ of this sample of 32 Galactic novae, which is devoid of any faint/fast types, is a *hard upper limit* to the completeness for our M51 survey: $\epsilon = 69$ percent.

5.2 Simulation II. M87 Novae

Next to our own Galaxy and M31, the massive elliptical galaxy M87 boasts the largest sample of densely observed nova light curves, the product of a two-month *HST* observing campaign (Shara et al. 2016). Due to the brevity of that survey, approximately half of those light curves are too incomplete for our simulation studies, but we were able to utilize 15 M87 novae whose observed light curves extend beyond t_2 . This dataset provides another independent test of the detection efficiency ϵ of the M51 survey, though faint/slow M87 novae were almost certainly missed. As in the case of the Galactic novae, this sample of M87 novae provides an independent *upper limit* on our M51 survey’s detection efficiency.

We computed the absolute magnitudes for the M87 novae assuming a distance $d = (16.4 \pm 0.5)$ Mpc, corresponding to a distance modulus of 31.1 mag (Bird et al. 2010). Each of the selected light curves was then begun at $t_0 = [-20, -19, -18, \dots, 345]$ days and sampled with the *HST* observing cadence. The final yield for the M87 novae was a set of 5,475 simulated nova light curves, which we then evaluated for detectability within the M51 search parameters.

Figure 6 (center) shows the results of our M87-based nova detection efficiency evaluations. With a mean of 34 percent, it falls between that of the Galactic and M31 novae, though much closer to the latter (see below). We note that although the M87 survey discovered a number of faint/fast novae (Shara et al. 2017) which would have significantly reduced the overall mean ϵ of the M51 survey, most of those novae were excluded from our simulations because their light curves either dropped below the *HST* detection limit too quickly, or were prematurely cut off during the decline period when the survey ended (the latter also occurred for a few of the brighter novae). Thus, as noted above, the $\epsilon = 34$ percent result for the M87 nova sample, applied to the M51 survey, is an *upper limit*.

5.3 Simulation III. M31 Novae

The most unbiased sample of novae available to us is that of M31. Unlike our own Milky Way, where dust extinction and reddening severely hampers our ability to detect distant novae in the plane of the Galactic disk, M31 affords us a clearer view of its stellar population. Given that the distances of these novae are all well determined and internal reddening is minimal, it is not surprising that our nearest massive galactic neighbor has yielded a significant number of “faint and fast” novae. As already noted, faint/fast novae are challenging to detect in external galaxies because they are often too faint to detect via ground-based observations, which are limited by poor weather

and seeing, bright moon, and easy-to-manage, “a few nights at a time” block scheduling of telescopes.

For this study, we utilized 29 novae observed during two M31 surveys that are among the most complete and unbiased available, because of their near-daily observing cadences over extended periods of time (Arp 1956; Kasliwal et al. 2011). We also added 30 well-sampled M31 nova light curves observed by the Zwicky Transient Facility (ZTF) between 2019-2021 (<https://irsa.ipac.caltech.edu/cgi-bin/Gator/nph-scan?projshort>). We excluded from consideration all novae in those surveys whose outburst peaks may have been missed. This brought our M31 sample size to 59, our largest extragalactic nova sample by far.

Absolute magnitudes for each of the M31 novae were calculated using a distance modulus of 24.32 mag (Wagner-Kaiser et al. 2015) and assuming a uniform extinction $E(B - V) = 0.062$ (Schlegel et al. 1998). Each light curve was initiated at $t_0 = [-20, -19, -18, \dots, 345]$ days and sampled with the *HST* M51 observing cadence. As with the Galactic novae, interpolation was utilized where small gaps in the light curves coincided with one of the M51 *HST* epochs. We were thus able to simulate a set of 21,535 realistic light curves using the M31 novae. Once again, the simulated light curves were evaluated for detectability within the M51 survey.

Figure 6 (right panel) shows the detection efficiency ϵ for the simulated M31 novae; as before, the M_{peak} , t_2 , and ϵ shown in the plot correspond to the “parent” nova that was used to generate the simulated light curves. Not surprisingly, many of the novae with brighter M_{peak} and longer t_2 still had higher overall detection rates than their fainter/faster counterparts. At 20.5 percent, the mean ϵ for the M31-based simulations was much lower than that of the Galactic-nova-based simulations, as expected given the significant subset of faint/fast novae in the less-biased nova sample of M31.

To quantify our completeness we carried out the following set of simulations. In each trial, we chose one of the M31 nova at random, initiated its outburst on a random day as described above, and analyzed its light curve to determine whether that nova was detectable within the M51 survey, using our V_{606} -band selection parameters. We continued selecting novae at random and evaluating them for detectability until the number detected, N_{obs} , reached 14. The “true” number of novae needed to reach $N_{obs} = 14$ during each trial was recorded as N_{tr} . These trials were repeated 10^5 times, yielding the distribution of $10^5 N_{tr}$ shown in Figure 7. The mean and 1-sigma (± 34.1 percent) widths of the N_{tr} distribution are 69^{+19}_{-15} novae, corresponding to a nova detection efficiency $\epsilon = 20.3^{+5.6}_{-4.3}$ percent.

The above value is in agreement with the mean detection rate of $\epsilon = 20.5$ percent for the full dataset of M31 simulations. The mean ϵ values for the ZTF, Arp (1956), and Kasliwal et al. (2011) subsets are also consistent, at 20, 22, and 18 percent, respectively.

6 DISCUSSION

6.1 Detection Efficiency and the True Nova Rate in M51

The simulations described in section 5 indicate that less than a quarter of the novae that underwent an outburst in M51 during the *HST* M51 survey were detected, *assuming that the nova populations of M51 and M31 are similar*. While it might be tempting to simply lump all of the M31, M87 and Galactic novae of Table 3 into a single simulation, we again emphasize that the most biased sample is that of the Galactic novae, which miss almost all faint, fast novae. Furthermore, as Figure 5 demonstrates, “fast” novae cannot be quantified by t_2 alone, since the light curve decline rate preceding

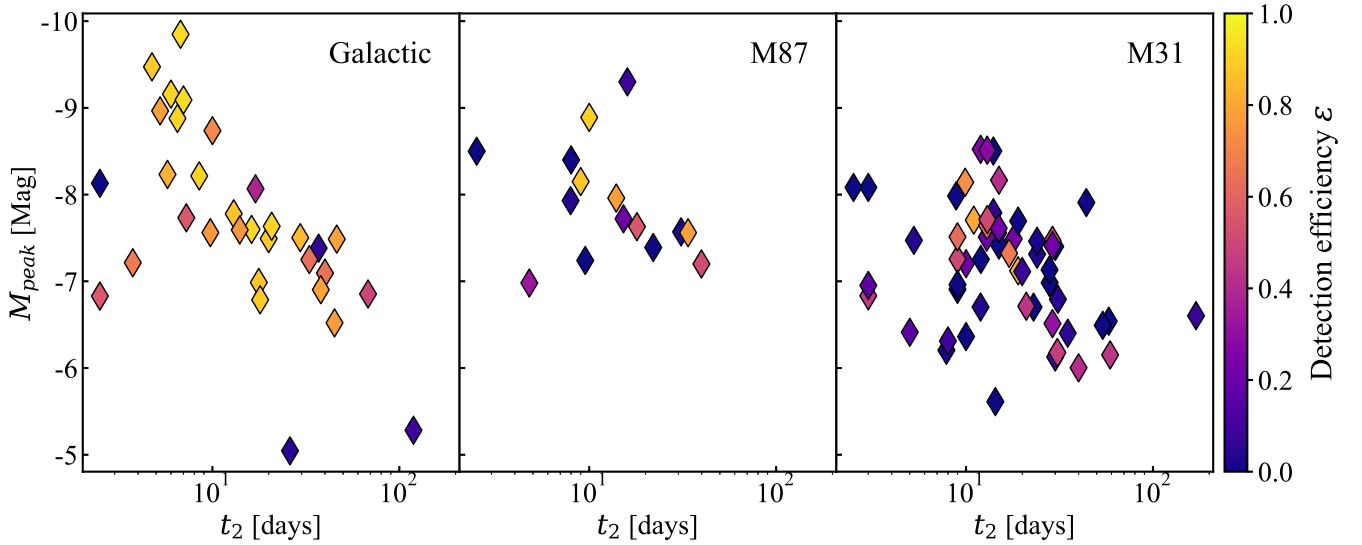


Figure 6. Detection efficiency ϵ for simulated light curves from Galactic (left), M87 (center), and M31 (right) novae. See Sections 5.1–5.3 in the text for details.

Table 2. Nova detection efficiency from simulations

Simulation	$\langle M_{peak} \rangle^a$ (Abs. mag)	$\langle t_2 \rangle^a$ (days)	Input Novae	Trials	% Detected (Mean ϵ)	Reference
Synthetic	-7.5	77	1071	370,566	$< 65^b$	This work
Galactic	-7.7	22	32	11,680	$< 69^c$	1
M87	-7.9	16	15	5,475	$< 34^d$	2
M31	-7.1	22	59	21,535	$20.3^{+5.6}_{-4.3}$	3, 4, 5

^a Parameters listed are averaged values from the distributions of observed *input* novae that the sets of simulated light curves were generated from.

^b This value is a strong upper limit since this simulation assigned equal weight to all simulated novae, including those with simultaneously large M_{peak} and t_2 ; no such novae are known to exist.

^c This value is a strong upper limit since Galactic surveys are strongly biased against the detection of faint/fast novae (see Section 6.3.1 for more).

^d This value is an upper limit since the M87 survey was biased against the detection of faint novae, and the fast novae that had been detected were largely excluded from our sample (Section 5.2).

References (for “input” nova light curves): (1) [Strope et al. \(2010\)](#); (2) [Shara et al. \(2016\)](#); (3) [Arp \(1956\)](#); (4) [Kasliwal et al. \(2011\)](#); (5) ZTF (<https://irsa.ipac.caltech.edu/cgi-bin/Gator/nph-scan?projshort=ZTF>).

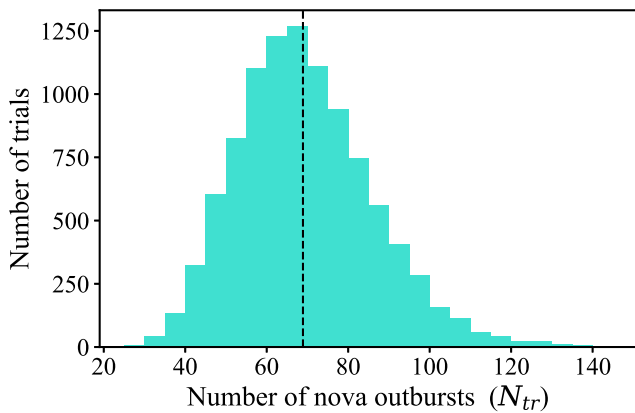


Figure 7. Distribution of the “true” number of (randomly sampled) novae, N_{tr} , required to recover the number of observed novae, $N_{obs} = 14$, in 10^5 trials. The dashed line marks the mean value of $N_{tr} = 69$ novae. $\frac{N_{obs}}{\langle N_{tr} \rangle} = 20.3$ percent, which best approximates the detection efficiency ϵ of our M51 nova survey if the nova populations of M31 and M51 are not very dissimilar.

and following the two-magnitude-decline point plays a much larger role in a nova’s detectability. This light curve *shape* effect is evident in Figure 6, where many of the M31 novae (right panel) have much lower detection efficiency than their Galactic counterparts (left panel) within the same $M_{peak} - t_2$ parameter space. That’s because the overall *shape* (especially the rapid declines) of many M31 nova light curves makes them difficult to detect in our own Galaxy. Theory and simulations ([Yaron et al. 2005](#)) predict that a similar population of faint/fast Galactic novae should exist. These Galactic novae have not yet been discovered because, *at minimum*, months-long, large area, \sim nightly *infrared* (to minimize reddening effects) surveys are required for their detection. Lumping the M87, M31 and Galactic novae underestimates the number of faint fast novae and overestimates our detection efficiency in M51. We adopt the detection efficiency ϵ yielded by our M31 simulations because we consider this estimate to be the most robust, given the relative size and lack of observational bias in that sample.

Figure 8 shows that the *K*-band light distribution in M51 (which follows the distribution of red giants with masses $\sim 1 M_{\odot}$) is in good agreement with the spatial distribution of novae in M51 (see Figure 3 for the area included in this analysis). This is consistent with the

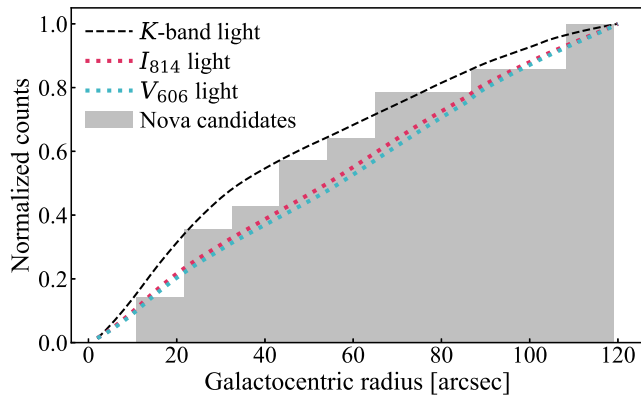


Figure 8. Luminosity profile of M51 in K -band (black), I -band (red), and V -band (blue) light. The cumulative distribution of nova candidates we identified in our survey is shown in grey. Note that this plot does not show all of M51’s light at these radii; it includes the fraction of the galaxy light (and detected novae) that overlap with this survey’s *HST*-observed area.

distribution of novae found in the massive elliptical galaxy M87, which was also shown to follow the K -band light (Shara et al. 2016).

As Figure 3 shows, our photometric catalog covered a region that encompasses ~ 40 percent of the K -band light from M51. To calculate this fraction, we first determined the amount of light in the area that consistently remained within the field of view of the *HST* survey, a circle of radius ~ 102 arcsec. We then subtracted the inner 10 arcsec, which was excluded from our photometric catalog because its high surface brightness and stellar density presents a challenge for typical photometry tools. We computed the fraction of M51 light included in our study under the assumption that the total light from M51 is encompassed within a circle of radius ~ 220 arcsec. We used a 2MASS K -band image to get the photon counts within the specified areas, yielding a fraction of ~ 40 percent of the M51 K -band light covered by this survey.

We now have in place the three key values needed to derive the M51 nova rate. These are:

- the fraction of M51’s light consistently observed in the *HST* campaign (Figure 3), 40 percent;
- the determination that the novae “follow the light” in M51 (Figure 8); and
- the nova detection efficiency for this *HST* campaign, $\sim 20.3^{+5.6}_{-4.3}$ percent.

Then, under the assumption that the underlying CV population in M51 resembles that of M31, we conclude that the intrinsic nova rate in M51 is 172^{+46}_{-37} novae yr^{-1} . This M51 nova rate is nearly an order of magnitude higher than previously claimed (Shafter et al. 2000).

6.2 Nova Rates and Distributions in Different Galaxy Types

Although binary population synthesis models have predicted that nova rates (ν , normalized by K -band luminosity L_K) should vary with Hubble type (Matteucci et al. 2003; Claeys et al. 2014; Chen et al. 2016), earlier ground-based surveys found little evidence for this (Shafter et al. 2000). Given that this survey confirms what several others have already suggested – that ground-based surveys tend to miss a large fraction of nova outbursts (Shara et al. 2016; Mróz et al. 2016) – it is now time to reevaluate the evidence.

Assuming a value of $L_K = 16.6 \times 10^{10} L_{\odot,K}$ for M51 (Shafter et al. 2000) and a rate of 172^{+46}_{-37} novae yr^{-1} , we find

a luminosity-specific nova rate (LSNR) of $\sim 10.4^{+2.8}_{-2.2}$ novae $\text{yr}^{-1}/10^{10} L_{\odot,K}$ for M51. Both rates are nearly an order of magnitude higher than the ground-based values from Shafter et al. (2000). Remarkably, Shara et al. (2016) found a luminosity-specific nova rate of $7.88^{+2.3}_{-2.6}$ novae $\text{yr}^{-1}/10^{10} L_{\odot,K}$ for M87, within the error range of our *HST*-derived rate for M51. The similarity of these values is inconsistent with Chen et al. (2016), who predicted an order-of-magnitude-higher LSNR value for M51-like galaxies than for M87-like elliptical galaxies. The best evidence now in hand demonstrates that the difference between the LSNRs of M87 and M51 may be much smaller than that predicted. Note that the M87 nova rate was conservatively calculated, assuming no incompleteness (Shara et al. 2016). Applying our incompleteness analysis to the M87 *HST* survey may well yield an even higher nova rate for that galaxy – even closer to the LSNR we observe for M51.

Figure 9 shows the published luminosity-specific nova rates for 13 different galaxies. While our newly extrapolated rate for M51 appears to be higher than those of the 12 other galaxies, this may not in fact be the case, as none of the other 12 nova rates were derived using our detailed detectability analysis. Comparable studies of other galaxies may well yield equally high luminosity-specific nova rates by improving incompleteness corrections. Similarly, high-cadence surveys will also increase nova rates universally, because more frequent observations lower incompleteness. Such is the case for M87 and the LMC, whose LSNRs are already higher than the 10 remaining galaxies’. Unlike most of the rates shown in Figure 9, the LSNRs for these two galaxies were extrapolated from surveys with near-daily cadence. Hence they can be considered far more reliable than their sparsely surveyed counterparts – particularly with respect to faint/fast novae.

6.3 Additional Uncertainties

The following is a discussion of the various uncertainties in our analysis, related to a) the selection of novae, and b) the detection parameters, that were used for the simulations described in Section 5.

6.3.1 Nova population differences between galaxies

Our analysis relies on several assumptions which are not definitive and which impact our final results. Chief among them is the assumption that the nova population in M51 resembles that of M31. As noted above, and shown in Table 2, assuming instead a nova population like that in our Galactic sample would result in a significantly higher detection efficacy for this survey, and consequently, a lower derived nova rate estimate. We repeat that the nova rate determined using the M31 dataset is almost certainly more reliable, given that the M31 sample a) includes faint-fast novae which are conspicuously absent from the Galactic sample, b) is compiled from unbiased³ surveys, and c) boasts a much larger sample size.

The survey efficiency results of the simulation based on M87 novae are more consistent with those derived from the M31 dataset than its Galactic counterpart. However, as Table 2 shows, that sample is biased towards the brighter novae. The larger distance to M87,

³ We sourced the M31 novae from surveys selected for their high cadence and long duration. Combined with the relatively (compared to our Galaxy) low variation in reddening and accurate distance to M31, which provided us with well-constrained absolute magnitudes, this resulted in the most unbiased sample available, as detailed in Section 5.3.

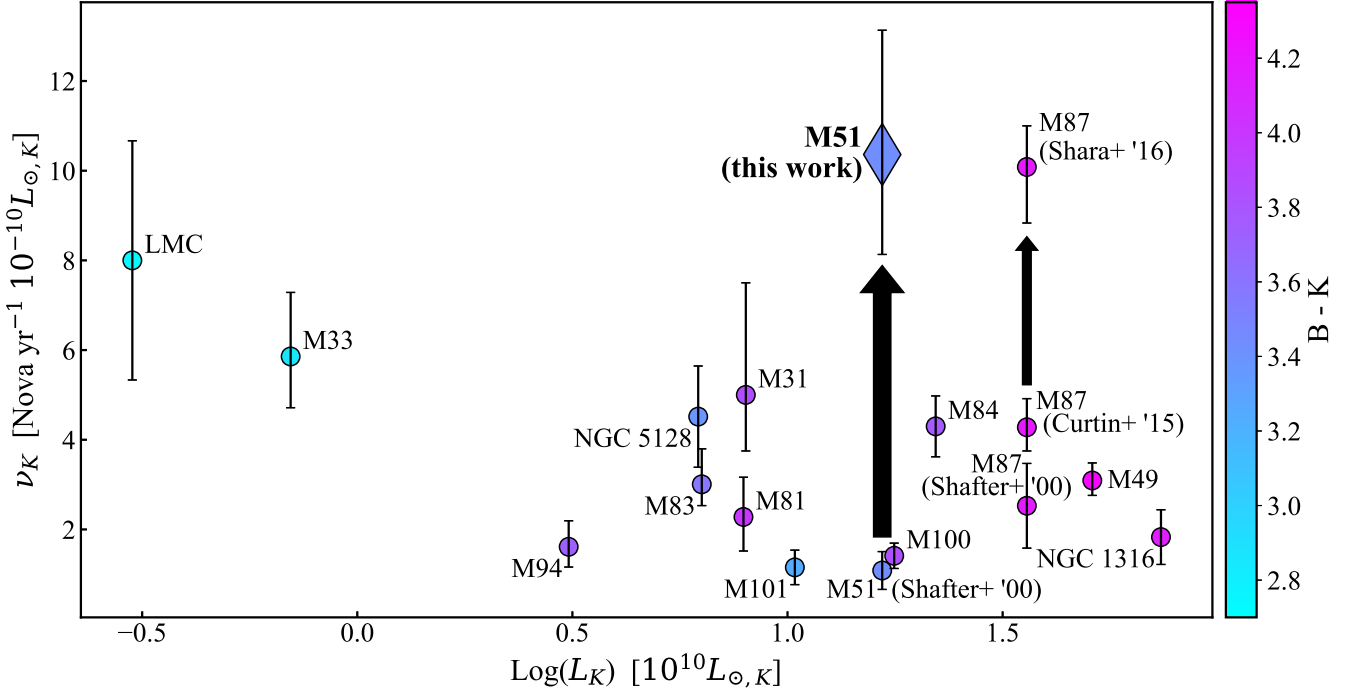


Figure 9. Luminosity-specific nova rates for an array of galaxies. All values are from Della Valle & Izzo (2020) (table 7), with the exception of M83 (which was taken from Shafter et al. (2021)), and the two galaxies with *HST*-based nova rates: M51 and M87. For the former, we adopted a *K*-band luminosity of $L_K = 16.6 \times 10^{10} L_{\odot,K}$ (Shafter et al. 2000). The larger black arrow highlights the difference between the previously published LSNR and our newly determined rate for M51 (diamond marker). The smaller arrow denotes the increase in LSNR for M87 established via the high-cadence *HST* survey by Shara et al. (2016), compared to earlier values calculated by Shafter et al. (2000) and Curtin et al. (2015) through ground-based studies.

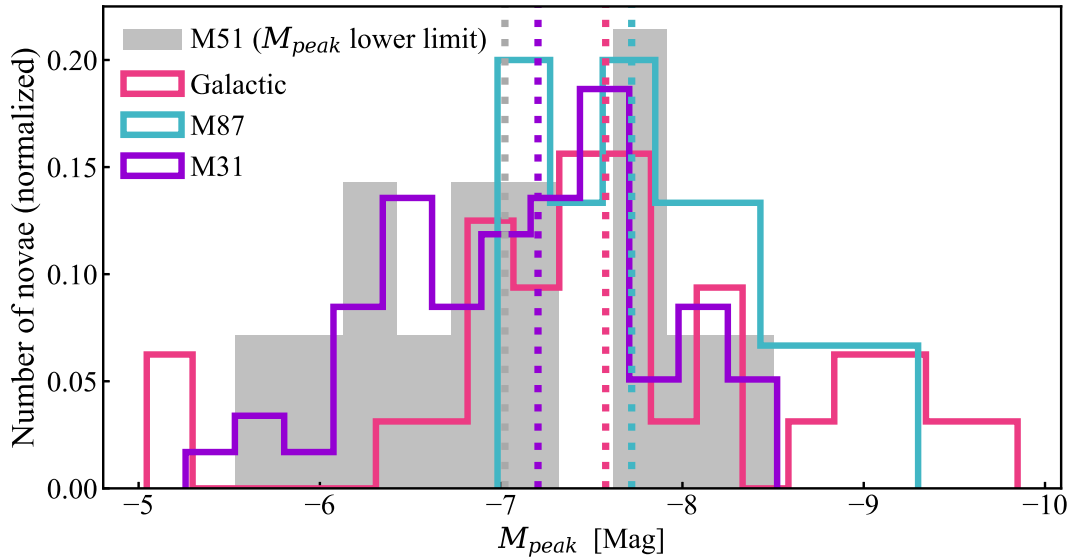


Figure 10. M_{peak} distributions for Galactic (pink), M31 (violet), M87 (blue), and M51 (grey) novae. For M51, all M_{peak} values are lower limits as the outburst “peaks” were likely missed for most novae due to the survey observing cadence. The dotted lines denote median values.

combined with the relatively short duration of the M87 *HST* survey, hampered the detection of well-sampled novae of longer duration and lower M_{peak} . We also note that as a massive elliptical galaxy with an overall older stellar population, the nova distribution in M87 may be different from that of its spiral counterparts... which is why we did not simply lump together the M31 and M87 nova samples.

Figure 10 shows the distributions of M_{peak} for the Milky Way (32 novae), M31 (59 novae), M87 (15 novae), and M51 (14 novae) sample light curves. Due to the large gaps between the *HST* observations of those novae; we can not determine their actual peak luminosities of those novae; we can only determine their lower limits. The fainter “tail” of the M87 nova distribution is deficient. We attribute this to observa-

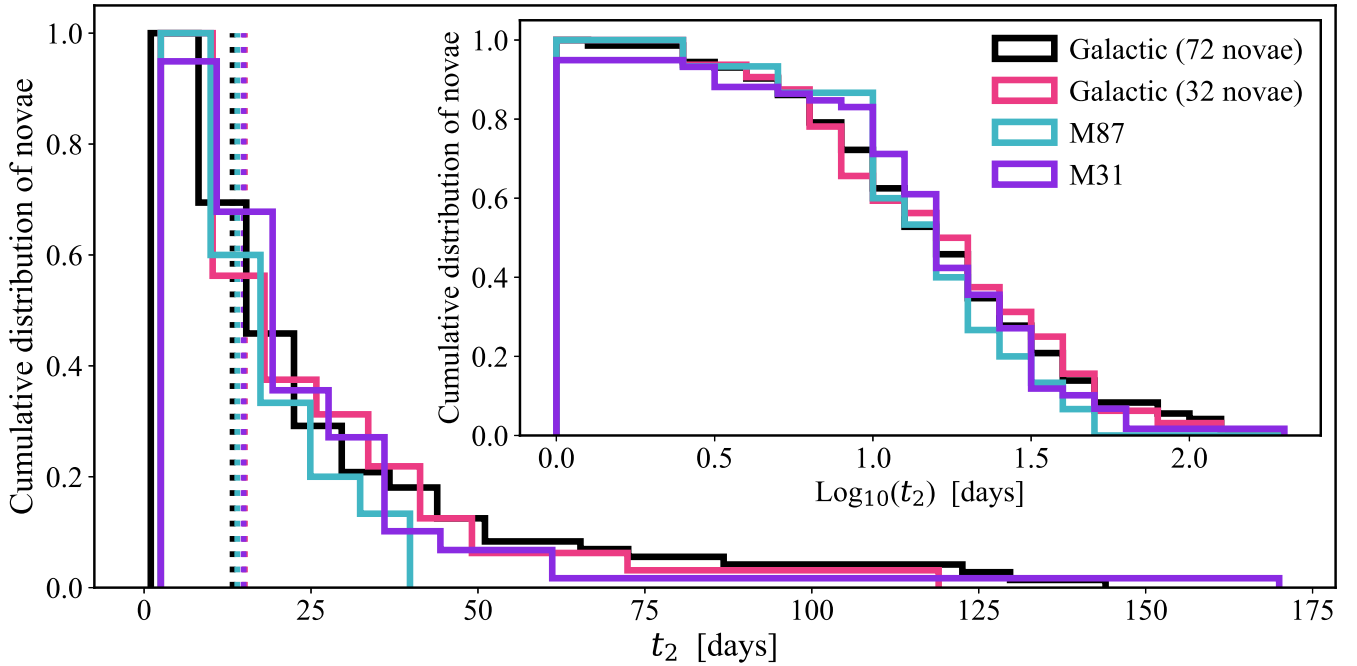


Figure 11. Cumulative t_2 distributions for Galactic (pink), M31 (violet), and M87 (blue) novae used in the simulations described in Section 5. A larger sample of Galactic novae, including 40 whose distances are not well constrained, is shown in black. Dotted lines denote the median values. The inset shows the distributions in log scale.

tional selection, i.e. the difficulty in detecting such faint novae, even with *HST*, at the distance of M87. In addition, the relatively short duration of that survey prevented the detection of slowly-declining novae, which have lower M_{peak} . The higher- M_{peak} tail of M51 is missing as well – again, not surprisingly – as one might expect from a survey with (on average) 10 day gaps, missing most luminous, fast novae near maximum luminosity.

Figure 10 also appears to show a dearth of Galactic novae with M_{peak} fainter than ~ -6.75 . This is at least partly due to a selection bias that favors the detection of brighter Galactic novae, as described in Section 5.1. Note that Özdönmez et al. (2018) and Shafter (2017) find a mean M_{peak} of -7.2 for a subset of Galactic novae. In the case of the former, novae with well-determined distances were selected; for the latter, it was predominantly novae from the Galactic bulge. Since our own selection criteria were stricter (requiring well-determined distances and well-sampled light curves), it is not surprising that the mean M_{peak} for our sample is higher (Table 2). This further supports our claim that the resulting detection efficiency ϵ for our limited Galactic sample is an overestimate. In contrast, the mean M_{peak} for our M31 sample is consistent with not only the abovementioned estimates for larger subsets of Galactic novae, but also the entire dataset of observed novae in M31 (Özdönmez et al. 2018; Shafter 2017) – and not just the limited subset of well-sampled novae from unbiased surveys included in our simulation. This consistency further supports our adaptation of the ϵ value yielded by the M31 simulations.

Perhaps even more telling are the distributions of t_2 in the different galaxies. Unlike the absolute magnitudes, t_2 values are well constrained for 72 Galactic novae, since the latter can be determined from apparent magnitudes, even when the distance to the source is unknown. As Figure 11 shows, the overall distribution of t_2 for the novae in our M31 dataset is similar to that of the Galactic novae. This is true both for the larger distribution of 72 novae and for the

subset of 32 novae (with well-constrained distance estimates) that we utilized in the simulations described in Section 5.1. This further indicates that our M31 sample is a good representation of the typical nova population within a barred spiral galaxy.

6.3.2 Visual identification (or mis-identification) of nova light curves

Of the approximately 1,000 preliminary nova candidates selected for visual inspection from the full M51 *HST* dataset, only 14 light curves were clearly those of transients. Given the appearance of many of the simulated light curves (described in Section 5), which were based on observed nova samples that included a broader variety of shapes, we have good reason to believe that a significant number of novae embedded in the M51 data went unidentified, because, upon review, their light curves did not resemble the canonical nova decline shapes (Section 3). We applied a similar visual test to a subset of the simulated light curves that were marked as “detected” by our nova selection parameters, and found that as many as half of those light curves do not pass the by-eye inspection. This indicates that our survey detection efficiency could be overestimated by a factor of two – and consequently, that the intrinsic M51 nova rate could well be double our estimate of 172^{+46}_{-37} novae yr^{-1} . Out of an abundance of caution, we decided against incorporating this aspect of our analysis into our results. But we note that the M51 nova rate of 172^{+46}_{-37} novae yr^{-1} is a conservative determination.

Another factor to consider is that the 14 nova candidates we identified haven’t been spectroscopically confirmed. In the unlikely event that a small subset of them are not actually novae, the extrapolated nova rate for M51 would be reduced. For example, if two of the 14 sources are *not* in fact novae, the rate would be decreased to ~ 148 novae yr^{-1} – which is still far higher than the previously published rate of 18 novae yr^{-1} (Shafter et al. 2000). However, we consider this

scenario highly improbable; of the two classes of variable massive stars that can reach luminosities equivalent to novae, Mira variables are far redder than our nova candidates, and luminous blue variables typically rise in luminosity over months to years, not days, as is the case for our sources.

6.3.3 Color limitations

Among the crucial selection parameters used to winnow nova candidates from the enormous photometric dataset of M51 was the color near maximum light. Most novae exhibit a “blue” color near maximum light of $V - I < 0.50$ mag, but this property is by no means universal. Since we lacked sufficient “color” data for most of the novae in our simulation samples, we did not employ this selection criterion for the simulated set. Therefore, the detection efficiency vis-à-vis the actual M51 *HST* data may be – once again – overestimated, and our derived nova rate consequently *underestimated*.

6.3.4 Under- (or over-) representation of faint/fast novae in simulated samples

The number of observed faint/fast nova light curves available to us is rather small. Given the difficulty in detecting such novae, their intrinsic ubiquity is nearly impossible to reliably determine from current data. In our analysis, we assumed that the novae contained in our M31 dataset constitute a representative sample, although faint/fast novae are likely underrepresented. We also cannot rule out that such faint/fast novae do not commonly occur in other galaxies, including M51 – though we consider it far more likely that their detection in M31 and M87 was a result of superior detection efficiency in those surveys (compared to Galactic ones).

6.3.5 Magnitude uncertainties

Our analysis assumed that extinction internal to M51 is negligible and approximately uniform. Similarly, for the M31 novae used in our simulations, we did not account for possible differential extinction. This could introduce additional errors in magnitude that were not incorporated into our analysis. However, we found that arbitrarily making all M31 light curves one magnitude fainter had no significant effect on the mean detection efficiency for the M31 simulations. This indicates that internal extinction effects are likely negligible.

We also note that the novae in our M31 dataset were observed in similar but not identical filters as the M51 *HST* novae. As noted above, varying the luminosity of our sample novae by up to one magnitude had no discernible effect on their overall detectability, so a slight shift in filter wavelength should not significantly influence our results.

7 CONCLUSIONS

We conducted a study of the nova rate in M51 using a year-long *HST* survey and realistic simulations to thoroughly test the nova detection efficiency ϵ of that survey. Our incompleteness simulations modelled the detectability of well-observed M31 novae with unprecedented detail. This allowed us to extrapolate M51’s intrinsic nova rate with an unparalleled degree of accuracy – under the assumption that the nova population in M51 resembles that of M31. We find that the nova rate in M51 is $\approx 172^{+46}_{-37}$ novae yr⁻¹, and its luminosity-specific nova rate is $\sim 10.4^{+2.8}_{-2.2}$ novae yr⁻¹/10¹⁰ $L_{\odot,K}$. Both these rates are nearly an

order of magnitude higher than the previous published value based on ground-based observations (Shafter et al. 2000). In contradiction to theoretical predictions of order-of-magnitude differences in LSNRs between elliptical and spiral galaxies, M51 and M87 appear to display \sim comparable LSNRs. The novae in M51 closely follow the *K*-band light distribution in that galaxy, similar to the novae of M87.

ACKNOWLEDGEMENTS

This work was supported by the National Science Foundation Graduate Research Fellowship Program under Grant No. DGE 2036197. Any opinions, findings, and conclusions or recommendations expressed in this material are those of the authors and do not necessarily reflect the views of the National Science Foundation. CC and PvD acknowledge support from NASA Grant HST-GO-14704.001. We would like to thank Jay Strader for his valuable critiques and suggestions, which helped to significantly improve an earlier draft of this paper.

facilities: HST(ACS), AAVSO, ZTF

DATA AVAILABILITY

The M51 photometry and simulation data underlying this article will be shared on reasonable request to the first author. The other photometry data are publicly available from the references provided in Table 2.

References

- Arp H. C., 1956, *AJ*, 61, 15
 Bird S., Harris W. E., Blakeslee J. P., Flynn C., 2010, *A&A*, 524, A71
 Chen H.-L., Woods T. E., Yungelson L. R., Gilfanov M., Han Z., 2016, *MNRAS*, 458, 2916
 Claeys J. S. W., Pols O. R., Izzard R. G., Vink J., Verbunt F. W. M., 2014, *A&A*, 563, A83
 Conroy C., et al., 2018, *ApJ*, 864, 111
 Curtin C., Shafter A. W., Pritchett C. J., Neill J. D., Kundu A., Maccarone T. J., 2015, *ApJ*, 811, 34
 De K., et al., 2021, *ApJ*, 912, 19
 Della Valle M., Izzo L., 2020, *A&ARv*, 28, 3
 Dolphin A. E., 2000, *PASP*, 112, 1383
 Hillman Y., Prialnik D., Kovetz A., Shara M. M., 2016, *ApJ*, 819, 168
 Hillman Y., Shara M. M., Prialnik D., Kovetz A., 2020, *Nature Astronomy*, 4, 886
 Hoffmann S. L., Mack J., et al. 2021, “The DrizzlePac Handbook”, Version 2.0. Baltimore: STScI, <https://hst-docs.stsci.edu/drizzpac>
 Kasliwal M. M., Cenko S. B., Kulkarni S. R., Ofek E. O., Quimby R., Rau A., 2011, *ApJ*, 735, 94
 Kawash A., et al., 2021, *ApJ*, 922, 25
 Matteucci F., Renda A., Pipino A., Della Valle M., 2003, *A&A*, 405, 23
 McQuinn K. B. W., Skillman E. D., Dolphin A. E., Berg D., Kennicutt R., 2016, *ApJ*, 826, 21
 Mróz P., et al., 2016, *ApJS*, 222, 9
 Özdönmez A., Ege E., Güver T., Ak T., 2018, *MNRAS*, 476, 4162
 Schaefer B. E., 2018, *MNRAS*, 481, 3033
 Schlegel D. J., Finkbeiner D. P., Davis M., 1998, *ApJ*, 500, 525
 Shafter A. W., 2017, *ApJ*, 834, 196
 Shafter A. W., Ciardullo R., Pritchett C. J., 2000, *ApJ*, 530, 193
 Shafter A. W., Curtin C., Pritchett C. J., Bode M. F., Darnley M. J., 2014, in Woudt P. A., Ribeiro V. A. R. M., eds, *Astronomical Society of the Pacific*

Conference Series Vol. 490, Stellar Novae: Past and Future Decades. p. 77

([arXiv:1307.2296](https://arxiv.org/abs/1307.2296))

Shafter A. W., et al., 2021, *ApJ*, **923**, 239

Shara M. M., et al., 2016, *ApJS*, **227**, 1

Shara M. M., et al., 2017, *ApJ*, **839**, 109

Strope R. J., Schaefer B. E., Henden A. A., 2010, *AJ*, **140**, 34

Wagner-Kaiser R., Sarajedini A., Dalcanton J. J., Williams B. F., Dolphin A.,
2015, *MNRAS*, **451**, 724

Yaron O., Prialnik D., Shara M. M., Kovetz A., 2005, *ApJ*, **623**, 398

APPENDIX A: NOVAE USED IN SIMULATIONS

Some of the Galactic novae listed in this table have two or more values of M_{peak} and t_2 reported in the literature. Where available, we took M_{peak} from the AAVSO data compiled by [Strope et al. \(2010\)](#), provided that the sampling was \sim daily around the clearly observed peak. We define t_2 as the time it took for the nova to decline from M_{peak} by two magnitudes. Given that the nova luminosity can change by as much as 1 – 2 mag over a timescale of hours, it is not surprising that near-simultaneous observations yielded different values. For consistency, and to reflect the fact that the *HST* M51 epochs were 2.2 ksec each (and therefore could have easily missed the absolute outburst “peak” even if the observation occurred on the day of peak brightness), we utilized the AAVSO values even when a higher M_{peak} was reported elsewhere.

Table A1: Novae Used in Simulations.

Nova	m_{peak} (mag)	t_2 (days)	Filter
M31 Novae			
M31 (Arp '56) 1	16.43	3.0	m_{pg}
M31 (Arp '56) 2	16.43	2.5	m_{pg}
M31 (Arp '56) 4	18.15	10.0	m_{pg}
M31 (Arp '56) 5	15.99	12.0	m_{pg}
M31 (Arp '56) 6	16.37	9.9	m_{pg}
M31 (Arp '56) 7	16.01	14.0	m_{pg}
M31 (Arp '56) 8	17.0	9.0	m_{pg}
M31 (Arp '56) 10	17.04	5.3	m_{pg}
M31 (Arp '56) 12	16.0	13.0	m_{pg}
M31 (Arp '56) 13	17.04	29.0	m_{pg}
M31 (Arp '56) 15	16.9	15.0	m_{pg}
M31 (Arp '56) 16	17.26	12.0	m_{pg}
M31 (Arp '56) 17	17.2	24.0	m_{pg}
M31 (Arp '56) 19	17.72	31.0	m_{pg}
M31 (Arp '56) 20	17.19	17.0	m_{pg}
M31 (Arp '56) 21	17.4	20.0	m_{pg}
M31 (Arp '56) 23	17.38	28.0	m_{pg}
M31 (Arp '56) 24	17.81	23.0	m_{pg}
M31 (Arp '56) 25	17.56	3.0	m_{pg}
M31 (Arp '56) 26	18.0	29.0	m_{pg}
M31 (Arp '56) 30	18.02	53.9	m_{pg}
M31N 2007-10a	17.55	9.0	g
M31N 2008-07b	18.9	14.4	g
M31N 2008-08c	17.1	29.0	g
M31N 2008-09a	17.8	21.0	g
M31N 2008-09c	16.8	13.0	g
M31N 2008-10b	18.1	5.0	g
M31N 2008-11a	18.2	8.0	g
M31N 2008-12b	17.05	24.0	g
ZTF21aagkzve	17.26	9.0	ZTF- g
ZTF21aagkzve	17.09	15.0	ZTF- r
ZTF21acbfmh	16.53	8.9	ZTF- g
ZTF21acbfmh	16.35	15.0	ZTF- r
ZTF21abjiotr	19.25	–	ZTF- g
ZTF21abjiotr	18.39	30.0	ZTF- r
ZTF20acstbfh	17.68	3.0	ZTF- g
ZTF20acplkub	18.89	–	ZTF- g
ZTF20acplkub	18.31	7.9	ZTF- r
ZTF20acoqrpm	16.81	11.0	ZTF- g
ZTF20acgigfo	17.6	9.0	ZTF- g
ZTF20acgigfo	17.0	12.9	ZTF- r
ZTF20acfucwr	16.95	14.9	ZTF- g
ZTF20acfucwr	17.02	18.0	ZTF- r
ZTF20abqhsxb	17.81	12.0	ZTF- r
ZTF19acxrihd	18.11	35.0	ZTF- g
ZTF19acxrihd	17.97	58.0	ZTF- r

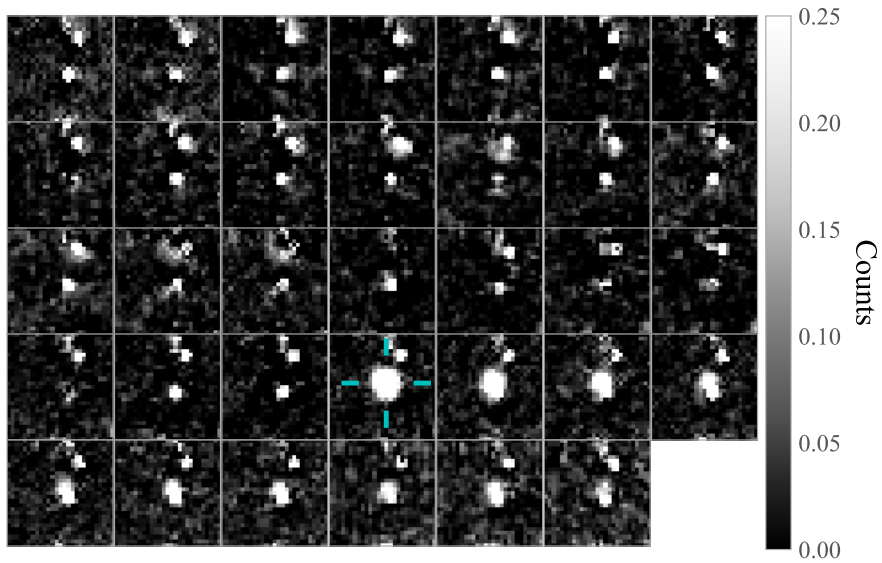
Nova	m_{peak}	t_2	Filter
ZTF19adakuos	17.53	28.0	ZTF-g
ZTF19adakuos	17.39	19.0	ZTF-r
ZTF19acqprad	18.51	40.0	ZTF-g
ZTF19acqprad	18.36	59.0	ZTF-r
ZTF19acnfsij	18.33	30.8	ZTF-r
ZTF19acgfhfd	17.11	30.0	ZTF-g
ZTF19acgfhfd	16.82	19.0	ZTF-r
ZTF19acfsteg	16.72	14.0	ZTF-g
ZTF19acfsteg	16.6	44.0	ZTF-r
ZTF19abirmkt	18.12	–	ZTF-g
ZTF19abirmkt	17.91	170.0	ZTF-r
ZTF19abfvpjh	17.31	10.0	ZTF-g
ZTF19abfvpjh	16.87	12.9	ZTF-r
M87 Novae			
1	21.84	16.0	V
2	22.25	10.0	V
3	22.64	2.5	V
4	22.74	8.0	V
5	22.99	9.0	V
6	23.18	14.0	V
7	23.21	8.0	V
9	23.42	15.2	V
10	23.51	18.0	V
11	23.57	31.0	V
12	23.58	33.8	V
15	23.75	22.0	V
19	23.9	9.5	V
20	23.94	39.8	V
23	24.16	4.8	V
Galactic Novae			
V356 Aql	6.97	37.0	V
V603 Aql	-0.5	5.8	V
V1370 Aql	7.7	9.8	V
V1494 Aql	4.11	8.5	V
V705 Cas	5.69	33.0	V
V723 Cas	7.08	17.0	V
V842 Cen	4.9	29.5	V
V476 Cyg	1.94	7.2	V
V1330 Cyg	9.9	119.0	V
V1974 Cyg	4.27	16.2	V
HR Del	3.58	68.0	V
DN Gem	3.58	13.0	V
DQ Her	1.56	40.0	V
V446 Her	4.83	17.7	V
V533 Her	3.0	20.0	V
CP Lac	2.02	6.0	V
DK Lac	5.9	18.0	V
IM Nor	7.84	26.0	V
RS Oph	4.94	6.8	V
GK Per	0.19	7.0	V
RR Pic	0.95	14.0	V
CP Pup	0.7	4.8	V
T Pyx	6.77	45.0	V
V3890 Sgr	8.05	5.2	V
U Sco	7.7	2.5	V
V992 Sco	7.7	10.0	V
FH Ser	4.5	46.2	V
V382 Vel	2.77	6.5	V
NQ Vul	6.19	2.5	V
PW Vul	6.41	3.8	V

Nova	m_{peak}	t_2	Filter
QU Vul	5.33	20.8	V
QV Vul	7.13	38.0	V

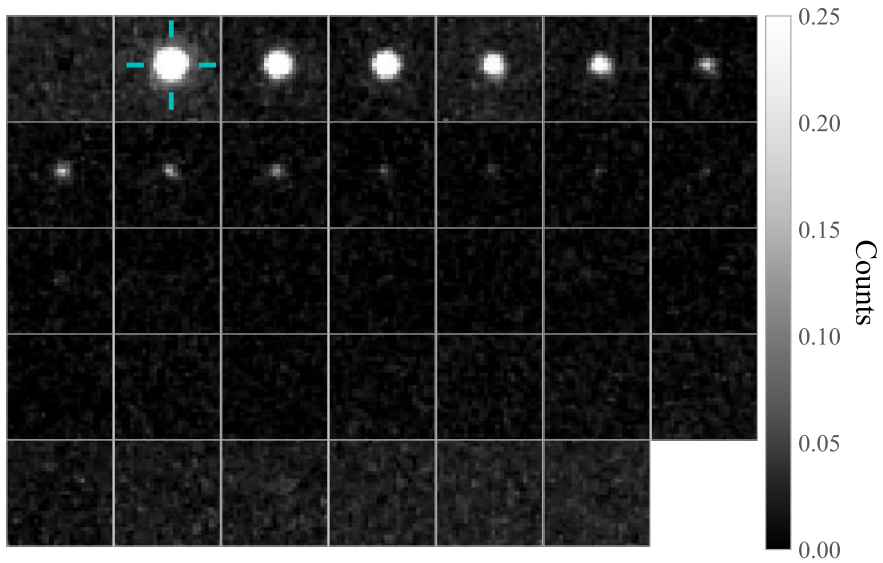
APPENDIX B: NOVAE IN DIFFERENCE IMAGES (“POSTAGE STAMPS”)

Figure B1 shows the 14 novae that we identified in M51, as they appeared in each observing epoch. To create these images, we first aligned the four dithered ACS images from each epoch using the `TWEAKREG` WCS alignment task and drizzled them together with `DRIZZLEPAC`, following the process described in Hoffmann et al. (2021). Separately, we created a composite image of M51 by “drizzling” together the individual images from all 34 epochs, again following the procedure described in Hoffmann et al. (2021). We then subtracted the composite image from each of the 34 individual drizzled images, creating the difference images shown below. This process allows us to clearly observe the appearance and decline of the novae. Each “postage stamps” cutout is 1 arcsec x 1 arcsec in size. Images corresponding to the epochs of observed peak luminosity are marked with cyan ticks.

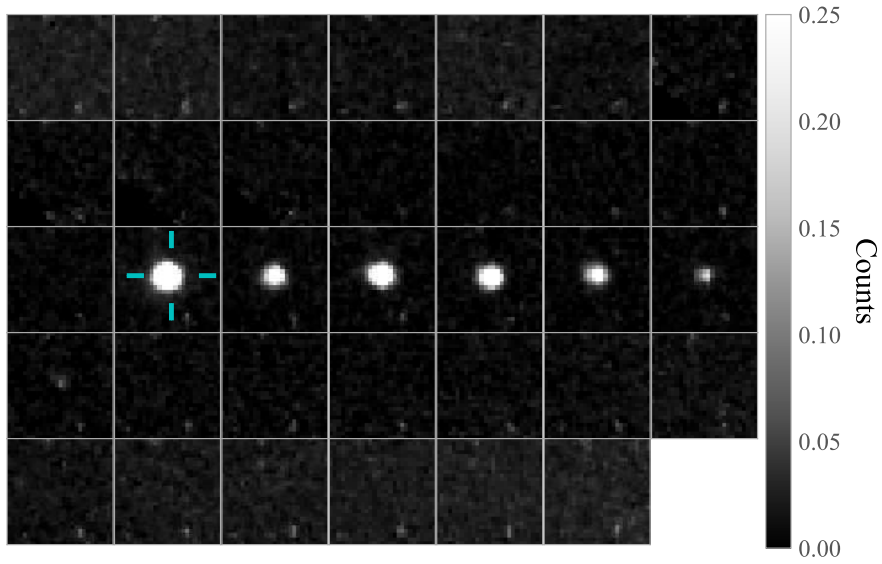
This paper has been typeset from a \LaTeX file prepared by the author.



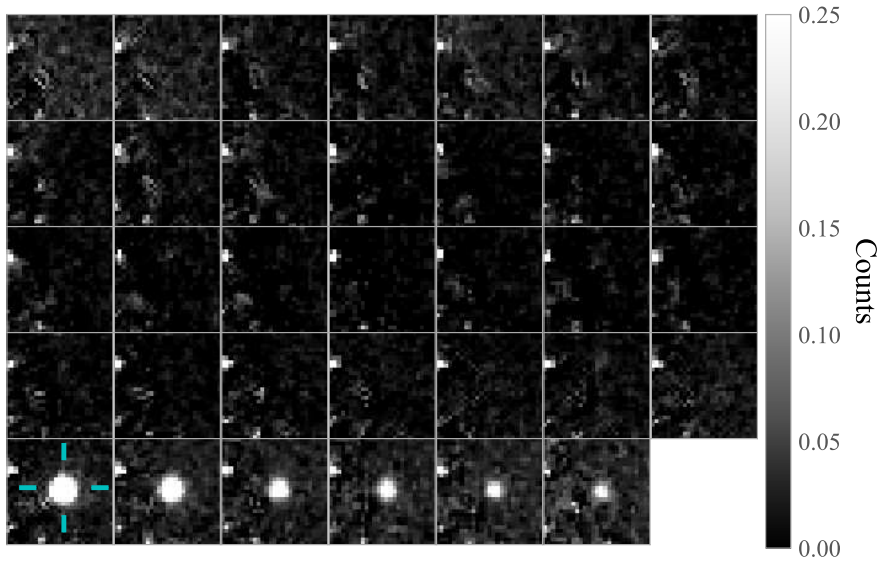
Nova 2



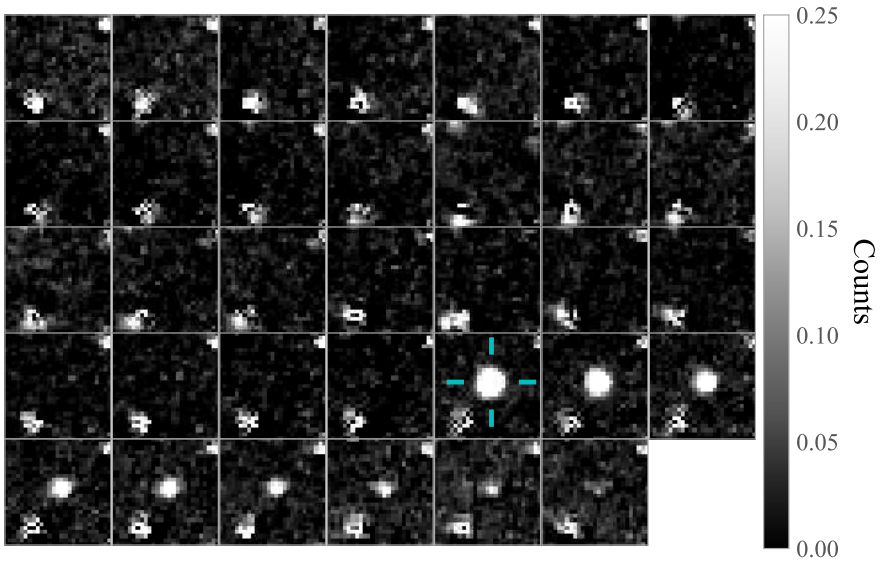
Nova 1



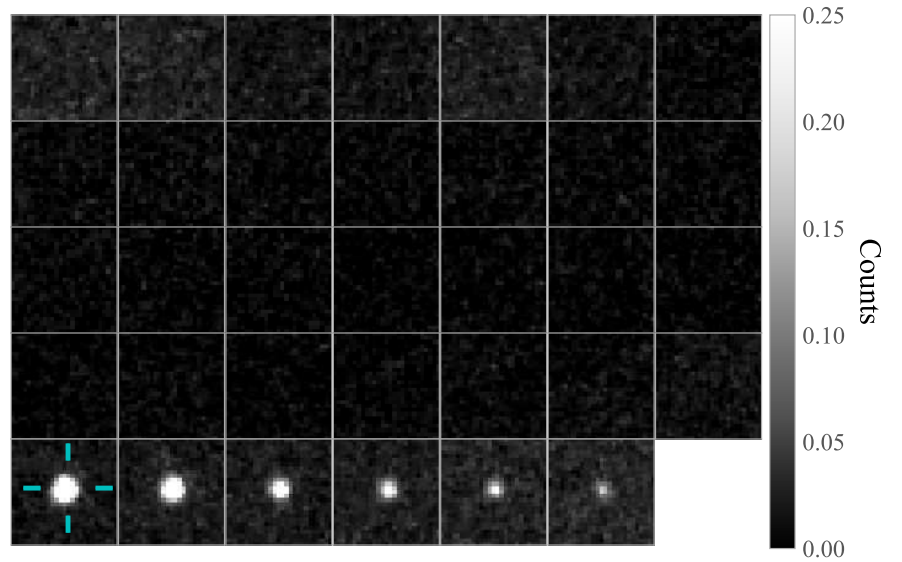
Nova 4



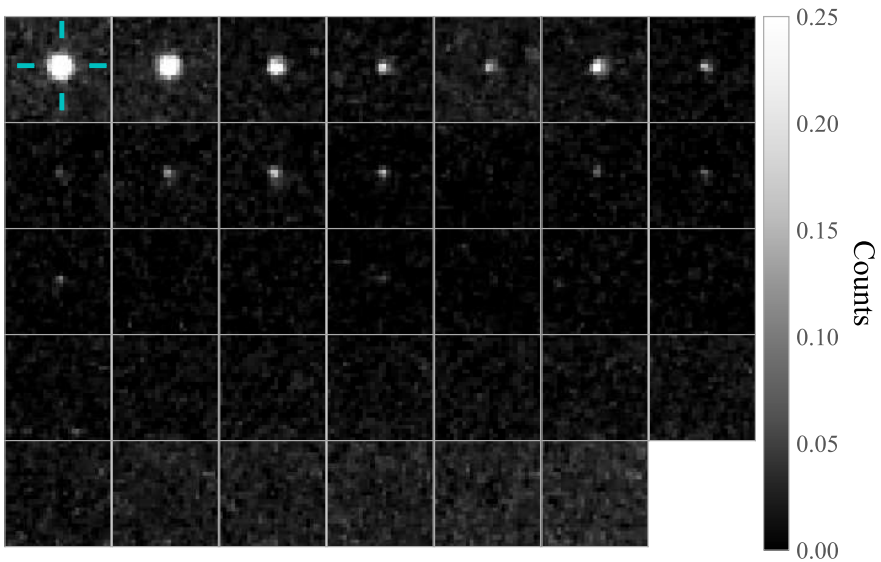
Nova 3



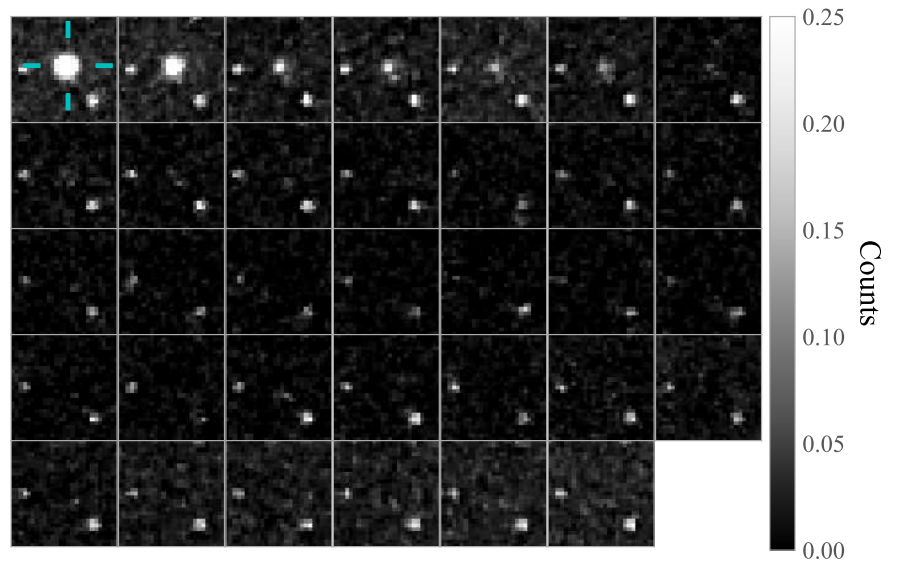
Nova 5



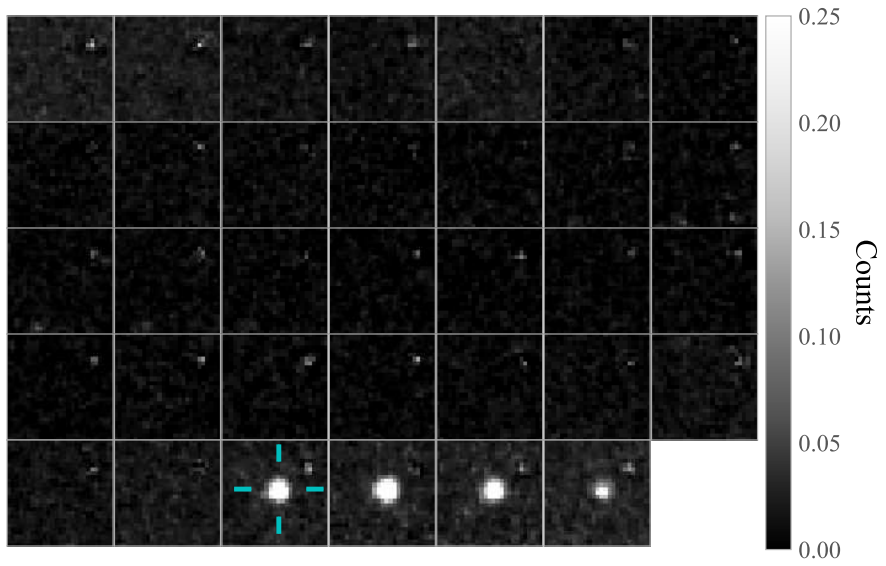
Nova 6



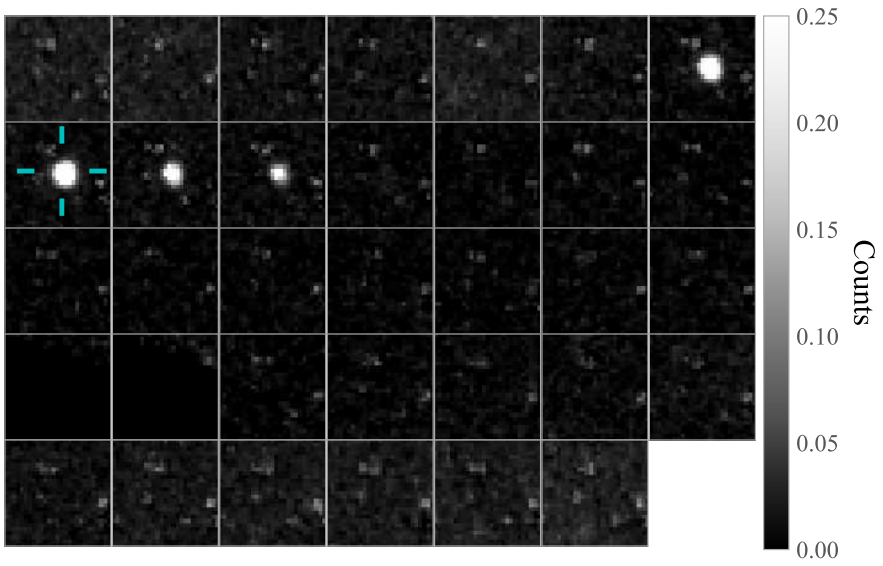
Nova 7



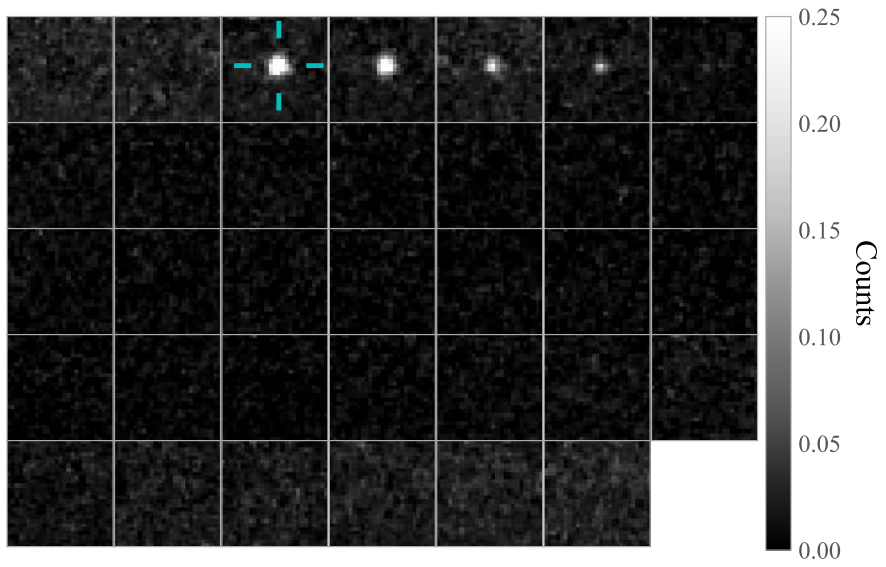
Nova 8



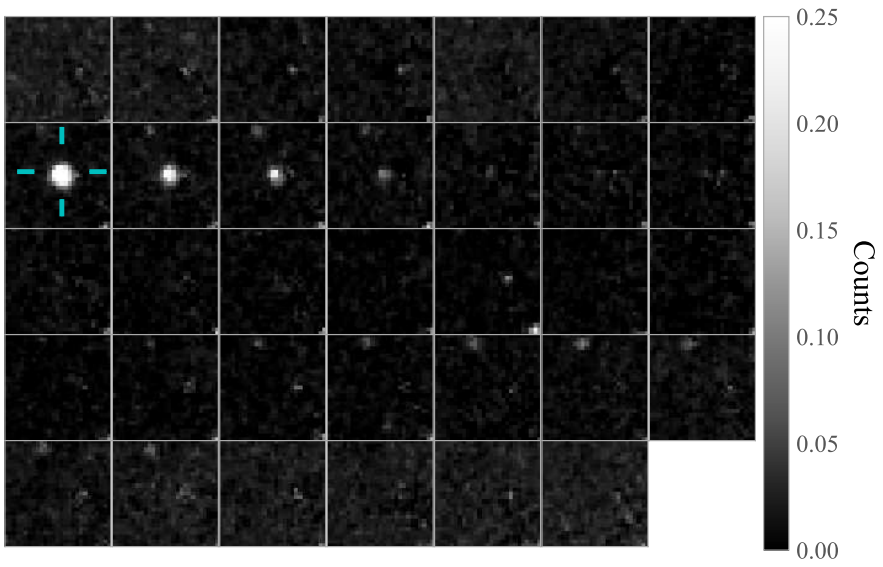
Nova 10



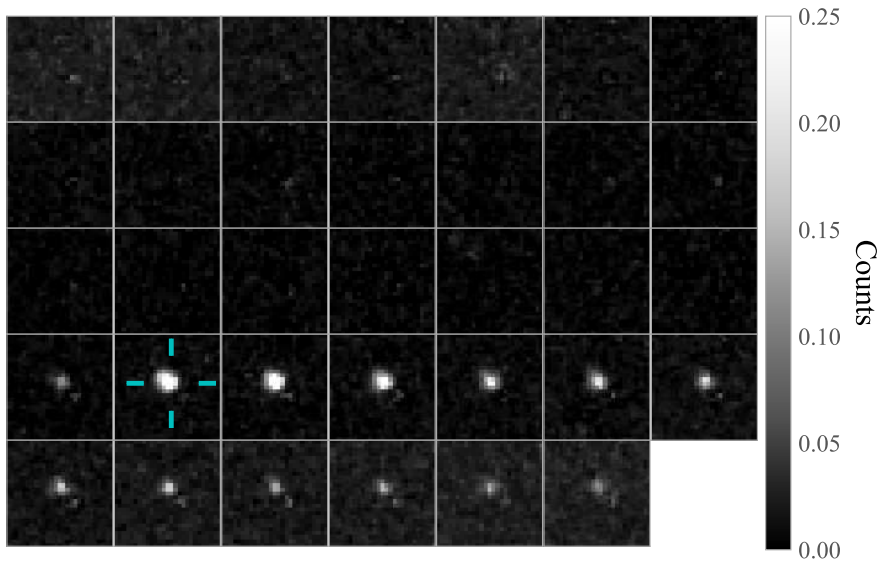
Nova 9



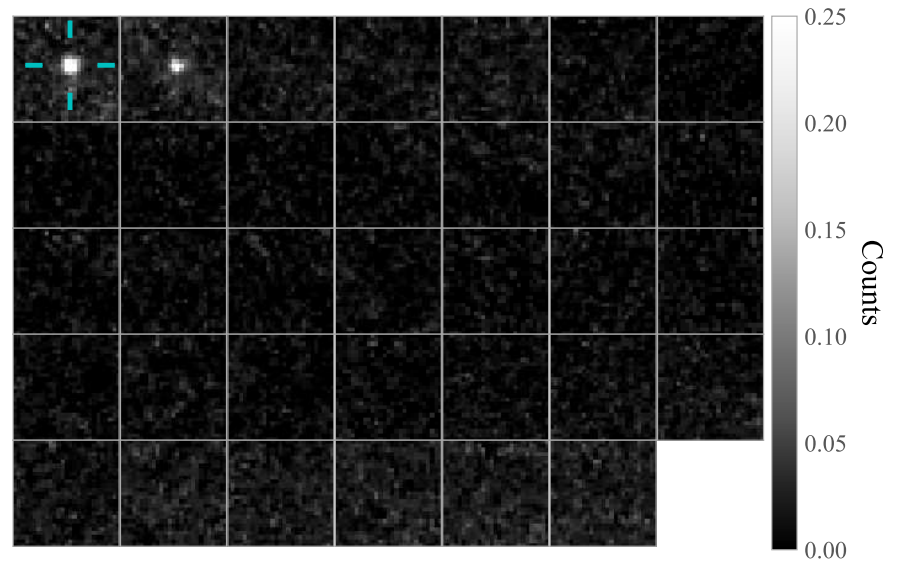
Nova 12



Nova 11



Nova 13



Nova 14

Figure B1: $1'' \times 1''$ V_{606} difference image cutouts of the 14 nova candidates in M51 for the 34 epochs of the *HST* observing campaign. Images corresponding to the epochs of observed peak luminosity are marked with cyan ticks.